Research Square

Preprints are preliminary reports that have not undergone peer review.
They should not be considered conclusive, used to inform clinical practice,
or referenced by the media as validated information.

Innovative Insights: Unveiling the Mechanism of Ginsenoside Re in Parkinson's Disease Therapy via BDNF/TLR4 Axis with Proteomics Approach

Mengjie Tang
Changchun University of Chinese Medicine
Fangyuan Zhang
Changchun University of Chinese Medicine
Ziqi Liang
Shanghai University of Traditional Chinese Medicine
Jing Tian
Changchun University of Chinese Medicine
Dean Guo
Shanghai University of Traditional Chinese Medicine
Jiyu Gong
Changchun University of Chinese Medicine
Wenyi Gao
Changchun University of Chinese Medicine
Zizhao Yang
zzyang@shutcm.edu.cn

Shanghai University of Traditional Chinese Medicine

Research Article

Keywords: Parkinson's Disease (PD), Brain Derived Neurotrophic Factor (BDNF), TLR4 Pathway, Ginsenoside Re (GsRe), Substantia Nigra Pars Compacta (SNpc), Dopamine (DA)

Posted Date: March 18th, 2026

DOI: https://doi.org/10.21203/rs.3.rs-8776159/v1

License: This work is licensed under a Creative Commons Attribution 4.0 International License.
Read Full License

Additional Declarations: No competing interests reported.

Abstract

Background

Brain derived neurotrophic factor (BDNF) is essential for neuronal survival, synaptic maintenance, and functional plasticity. Nevertheless, its specific pathophysiological role, particularly in the context of dopaminergic neurodegeneration and neuroimmune dysregulation in Parkinson's disease (PD), remains incompletely defined. Ginsenosides (GSs), bioactive triterpenoid saponins derived from Panax ginseng, exhibit broad neuroprotective properties across preclinical models of neurodegeneration; however, the identity of their principal pharmacologically active constituents and the precise molecular mechanisms governing their modulation of neuroinflammatory pathways in PD are still insufficiently characterized.

Purpose

This study seeks to elucidate the functional consequences of BDNF deficiency in PD related neurodegeneration and neuroinflammation. Then, systematically evaluate the therapeutic efficacy of ginsenosides in an established PD model as well as identify the dominant bioactive monomer and rigorously define its mechanism of action, with emphasis on BDNF dependent regulation of microglial activation and downstream inflammatory signaling.

Methods

A multimodal strategy integrating in silico network pharmacology with vivo and vitro experimental validation was elected. A well characterized MPTP induced murine model of PD was employed for vivo studies. Comprehensive assessments included longitudinal behavioral testing (rotarod, pole test, open field), immunohistochemical quantification of tyrosine hydroxylase (TH) positive neurons in the substantia nigra pars compacta (SNpc) and striatal dopamine terminals, ELISA based cytokine profiling, immunoblotting of key signaling proteins (e.g., TrkB, p-NF-κB p65, IκBα, STAT1, caspase-3) and quantitative proteomic analysis of the nigrostriatal pathway. Additional vitro experiments utilized MPP^+ treated primary mesencephalic neurons and BV2 microglial cells to dissect cell type specific mechanisms.

Results

Network pharmacology predicted BDNF as a central node linking ginsenoside targets to neuroinflammatory and anti-apoptotic pathways, hypotheses robustly confirmed experimentally. Ginsenoside Re (GsRe) was identified as the most potent and pharmacokinetically favorable monomer, demonstrating superior blood brain barrier permeability and selective accumulation in the SNpc and striatum. Mechanistically, GsRe enhanced BDNF expression and potentiated BDNF mediated suppression of TLR4 signaling, leading to downregulation of WDFY1, a critical adaptor facilitating TRIF dependent NF-κB/STAT1 activation. This cascade inhibition attenuated microglial pro-inflammatory polarization, reduced caspase-3 mediated neuronal apoptosis, preserved dopaminergic integrity, and significantly improved motor function in PD mice.

Conclusion

The BDNF/TLR4/WDFY1 axis as a pivotal regulatory hub in PD associated neuroinflammation was established and GsRe as a mechanistically grounded, brain penetrant candidate for disease modifying intervention was identified. These results advance the understanding of natural product mediated neuron microglia crosstalk and provide a rational framework for developing targeted therapeutics that restore neuroimmune homeostasis in PD and related disorders.

Highlights

(1) BDNF deficiency exacerbates the pathological progression of PD and the BDNF/TLR4 axis has been identified as a key mediator of neuroinflammation.

(2) GsRe penetrates key brain regions (substantia nigra, striatum) and ameliorates neuroinflammation, dopaminergic neuron degeneration and motor dysfunction in the MPTP-induced PD mouse model.

(3) GsRe synergistically inhibits TLR4 mediated microglial activation and downstream neuroinflammatory cascades by enhancing the inhibitory effect of BDNF on TLR4 and suppressing WDFY1 activity, thereby regulating neuroimmune homeostasis.

Introduction

Ginseng (Panax ginseng), the root of Panax ginseng C.A. Meyer (Araliaceae), exhibits multi-target pharmacological activities and holds therapeutic potential for a wide range of diseases, including central nervous system disorders, infectious diseases, and metabolic disorders. Ginsenosides (GS), a class of naturally occurring steroid like compounds in ginseng, have been extensively studied for their anti-inflammatory and antioxidant properties, as well as their ability to enhance mitochondrial function, regulate autophagy, and modulate apoptosis, collectively contributing to their efficacy in treating neurodegenerative conditions. GsRg1 has been demonstrated to ameliorate cognitive deficits and neuronal injury in vascular dementia by modulating the Adcy1/KDR mediated cholinergic synaptic transmission and activating the PI3K-AKT signaling pathway[1]. GsRc promotes mitochondrial biogenesis and exerts neuroprotective effects[2]. GsRo alleviates cognitive dysfunction and neuroinflammation in APP/PS1 transgenic mice through regulation of the IBA1/GFAP/MAPK pathway[3]. Based on their aglycone structures, GS are classified into three main types: dammarane type, oleanane type, and ocotillo type.

Although structurally diverse, GS share a common steroid saponin aglycone backbone, which underlies their shared pharmacological tendencies. Neuroprotection represents one of the most prominent and consistently observed properties across this class of compounds. The majority of GS exert neuroprotective effects through multiple mechanisms, including attenuation of oxidative stress, suppression of neuroinflammation, inhibition of apoptosis, modulation of neurotransmitter systems, and

upregulation of neurotrophic factor expression, collectively contributing to their potential in mitigating neurodegenerative disorders such as Alzheimer's disease (AD) and Parkinson's disease (PD).

Ginsenoside Re (GsRe), a representative member of protopanaxatriol type GS, exhibits significant advantages in neuroprotection, anti-inflammatory activity, and metabolic regulation owing to its distinctive C-6 hydroxyl group and disaccharide side chain. Accumulating evidence indicates that GsRe attenuates oxidative stress through activation of the Nrf2/GPX4 pathway[4], suppresses the NLRP3 inflammasome[5], and ameliorates neuroinflammation by inhibiting AMPKα1/STING signaling[6]. Furthermore, GsRe enhances synaptic plasticity via upregulation of Brain derived neurotrophic factor (BDNF)/TrkB signaling[7] and modulates PINK1 mediated mitophagy, demonstrating robust neuroprotective effects in models of AD, PD and other neurodegenerative disorders[8]. In addition, GsRe exerts beneficial effects in metabolic and cardiovascular disorders through PPARγ activation and modulation of the eNOS/NO pathway. Its ability to engage multiple synergistic targets positions GsRe as a promising therapeutic candidate for neurodegenerative diseases.

PD is a neurodegenerative disorder characterized by the progressive degeneration of dopaminergic neurons in the substantia nigra pars compacta (SNpc) and the intracellular aggregation of α-synuclein (α-syn) into Lewy bodies[9]. Its pathogenesis is highly complex. BDNF, a key member of the neurotrophic family, serves as a central regulator of the survival, differentiation, and synaptic plasticity of dopaminergic neurons within the nigrostriatal pathway[10, 11]. Accumulating evidence indicates that reduced BDNF levels are implicated in the pathological mechanisms underlying PD[12]. The aggregation of α-syn reduces BDNF expression and disrupts its axonal transport[13]. Concurrently, downregulation of BDNF relieves the transcriptional repression of α-syn, thereby promoting its abnormal accumulation [14]. Accumulated α-syn further binds to the TrkB receptor, establishing a negative feedback loop that exacerbates neuronal dysfunction[15]. Moreover, reduced BDNF levels lead to decreased expression of tyrosine hydroxylase (TH), the rate limiting enzyme in dopamine synthesis, which diminishes neuronal excitability and consequently impairs dopamine production and release[16, 17]. Emerging evidence indicates that neuroinflammation and immune system dysregulation are central to the pathogenesis of PD, with the Toll like receptor (TLR) family, particularly TLR4, playing a pivotal role in mediating these processes[18]. In early PD, TLR4 activation enhances microglial phagocytosis of α-syn, potentially delaying disease progression[19]. However, under chronic inflammatory conditions, sustained TLR4 signaling triggers excessive activation of the NF-κB and p38 MAPK pathways, amplifying neuroinflammatory responses and oxidative stress, ultimately leading to dopaminergic neuron apoptosis[20, 21]. In the MPTP induced PD model, TLR4 deficiency attenuates dopamine depletion, restores expression of tyrosine hydroxylase and dopamine transporter (DAT), modulates the activity of transcription factors NF-κB p65 and AP-1, and suppresses astrocyte proliferation[20, 22]. Notably, IL-1β and TNF-α released upon TLR4 activation have been shown to downregulate BDNF mRNA stability via p38 MAPK pathway activation[23, 24]. Neuronal activation of TLR4 suppresses BDNF expression, and selective TLR4 antagonists have been shown to restore impaired BDNF signaling[25]. BDNF exerts

feedback regulation on the TLR4 pathway: through TrkB receptor activation, BDNF stimulates the downstream NF-κB signaling cascade of TLR4, thereby promoting neuronal survival and synaptic plasticity[26]. Concurrently, BDNF attenuates excessive microglial secretion of inflammatory mediators and downregulates TLR4 and NF-κB expression, offering protection against neuroinflammatory damage in the central nervous system[27]. This bidirectional regulatory interplay holds significant implications for PD pathogenesis. Clinical studies demonstrate that BDNF levels in the cerebrospinal fluid of PD patients are significantly inversely correlated with TLR4 activity[28, 29], suggesting that dysregulation of the TLR4/BDNF axis may constitute a key mechanism underlying neurodegeneration in PD. Nevertheless, the causal relationship between these two molecules and the exact architecture of their regulatory network remain to be fully elucidated.

Emerging evidence indicates that GsRe possesses distinct regulatory properties within the neuroimmune system. GsRe exerts positive modulation on the BDNF signaling pathway. In a reserpine induced mouse model of depression, administration of GsRe significantly elevates BDNF protein levels in the hippocampus and activates downstream TrkB mediated CREB phosphorylation, thereby promoting neurogenesis[30]. On the other hand, GsRe demonstrates potent anti-inflammatory effects by suppressing the TLR4/NF-κB signaling pathway, effectively attenuating lipopolysaccharide (LPS) induced microglial activation[31]. These findings suggest that GsRe may concurrently target two critical pathological axes, neurotrophic support and neuroinflammation. Nevertheless, whether GsRe confers therapeutic benefits in PD through specific regulation of the BDNF/TLR4 axis remains unclear. Building upon this evidence, we propose a novel scientific hypothesis: BDNF deficiency acts as an upstream driver of aberrant TLR4 pathway activation in PD models, and the core therapeutic mechanism of GsRe may involve modulation of the BDNF/TLR4 axis to restore neuroimmune homeostasis.

To test this hypothesis, we employed MPTP induced wildtype and BDNF conditional knockout mouse models of PD to systematically investigate the therapeutic effects and underlying mechanisms of GsRe. We found that BDNF deficiency leads to aberrant activation of the TLR4 pathway and exacerbates PD related neuropathology. Notably, GsRe effectively reversed the hyperactivation of TLR4 signaling, compensated for neurotrophic deficits, and consequently restored neuroimmune homeostasis, thereby exerting robust neuroprotective effects. This study unveils, for the first time, a novel mechanism through which GsRe alleviates neuroinflammation in PD by modulating the BDNF/TLR4 axis. These findings not only provide direct evidence for the functional crosstalk between neurotrophic factors and immune receptors but also establish a solid experimental basis for developing new therapeutic strategies targeting the neural immune regulatory circuit in PD.

Materials and Methods

Chemical Reagents

GS were obtained from Shanghai Yuan Ye Biotechnology Co., Ltd. (batch number: J03GS153706); ginsenosides Rg1 ($C_{42}H_{72}O_{14}$, batch number: JB263899), GsRe ($C_{48}H_{82}O_{18}$, batch number:

O21IS229576), Rb1 ($C_{54}H_{92}O_{23}$, batch number: N18GB163839), Rd ($C_{48}H_{82}O_{18}$, batch number: JB238591), Rf ($C_{42}H_{72}O_{14}$, batch number: P25F12L140073), Rg2 ($C_{42}H_{72}O_{13}$, batch number: JB266498), Rc ($C_{53}H_{90}O_{22}$, batch number: N27HB202514), and Ro ($C_{48}H_{76}O_{19}$, batch number: A02IB211532) were also purchased from the same company. Chromatic grade acetonitrile and methanol were acquired from Fisher Scientific (Pittsburgh, PA, USA). Carbidopa and Levodopa Sustained Release Tablets (Carbidopa 50 mg and Levodopa200 mg/tablet) were purchased from MSD (Hangzhou MSD Pharmaceutical Co., LTD., Hangzhou, China)

The Chemical Composition of GS was Separated and Analyzed Using the UHPLC-Q-Orbitrap-MS/MS Method

Qualitative analysis was performed using UHPLC-Q-Orbitrap-MS/MS. A precisely weighed amount of 30.0 mg of GS powder was dissolved in 70% methanol, diluted to 10.0 mL, and sonicated to ensure complete dissolution. The solution was then filtered through a 0.22 μm microporous membrane prior to injection. Chromatographic separation was achieved on a Waters ACQUITY UPLC BEH C18 column (2.1 mm × 100 mm × 1.7 μm) with a mobile phase consisting of 0.1% formic acid in water (A) and acetonitrile (B) at a flow rate of 0.3 mL/min. The injection volume was 2 μL. The gradient elution program was as follows: 0–12 min, 82–80% A; 12–14 min, 80–70% A; 14–24 min, 70–68% A; 24–29 min, 68–67% A; 29–49 min, 67–25% A; 49–55 min, 0–82% A; 55–60 min, 82–82% A. The column temperature was maintained at 35°C. Mass spectrometric detection was carried out using an electrospray ionization (ESI) source in negative ion mode. The sheath gas flow rate was set to 35 Arb, the auxiliary gas flow rate to 10 Arb, and the sweep gas flow rate to 1 Arb. The S-Lens RF level was set to 55%, the capillary voltage to −3.5 kV, and the capillary temperature to 350°C. Full-scan MS data were acquired over a mass range of m/z 150 to 2000 with a resolution of 70,000, an automatic gain control (AGC) target of 3×10^6, and a maximum injection time of 100 ms. For MS/MS acquisition, the resolution was set to 17,500. The AGC target was set to 1×10^5, the injection time (IT) was 50 ms, with five data dependent MS/MS cycles per full scan, a precursor isolation window of 4.0 m/z, and a normalized collision energy (NCE) range of 25–55.

Quantitative Determination of GsRe and Dopamine via UHPLC-MS/MS

Sample analysis was performed using a Waters Xevo TQ-XS Triple Quadrupole Mass Spectrometer. For serum samples, 100 μL was used. Tissue samples were homogenized with 5 volumes of normal saline, and 100 μL of the supernatant was collected. 20 μL of DHBA or GsRc solution was added as an internal standard, followed by protein precipitation using 0.1% formic acid in acetonitrile. The supernatant was then dried under a nitrogen stream and reconstituted in 20 μL of 0.2% formic acid in methanol (8:2, V/V) before analysis. The chromatographic separation was carried out on an ACQUITY UPLC® BEH C18 column (50 mm × 2.1 mm, 1.7 μm) with a mobile phase consisting of acetonitrile (A) and 0.1% formic acid in water (B). Dopamine (DA) was acquired in positive ion mode with the following elution program: 0–2.5 min, 5% A; 2.5–4 min, 5%–20% A; 4–7 min, 20%–60% A; 7–7.5 min, 60%–5% A; 7.5–10 min, 5% A. The injection volume was 3 μL, and the flow rate was 0.2 mL/min. GsRe was acquired in negative ion

mode with the following elution program: 0–9 min, 12%–90% A; 9–12 min, 12% A. The injection volume was 3 μL, and the flow rate was 0.4 mL/min.

Network Pharmacology

Target information for GS was retrieved from the CTD and ChEMBL databases. Additionally, SMILES identifiers obtained from PubChem were submitted to the Swiss Target Prediction database to predict and supplement potential targets. These results were integrated to compile a comprehensive target profile of GS. PD–related targets were collected from OMIM, DisGeNET, and GeneCard databases. Overlapping targets between GS and PD were identified using Venn diagram analysis. The intersecting genes were imported into the STRING database to construct a protein–protein interaction (PPI) network, which was subsequently visualized and refined in Cytoscape software. Core targets were identified using the CentiScaPe 2.2 plugin based on topological analysis. Functional enrichment analyses, including Gene Ontology (GO) and Kyoto Encyclopedia of Genes and Genomes (KEGG) pathway annotations, were performed on the shared targets using the DAVID database. Finally, active components of GS, key targets, and the top 20 enriched KEGG pathways were integrated into Cytoscape 3.9.0 to generate a comprehensive active component/target/pathway/PD network for systematic visualization.

Molecular Docking

The crystal structure of BDNF (PDB ID: 1BND) was retrieved from the Protein Data Bank (PDB). The 3D structures of ginsenoside active components were obtained from the Traditional Chinese Medicine Systems Pharmacology (TCMSP) database. The protein file was imported into PyMOL software, where redundant ligands and water molecules were removed. Hydrogen atoms were added, charges were assigned, and the protein was set as the receptor before being saved in PDBQT format for subsequent use. Molecular docking was performed using AutoDock Vina 2.1.6. Upon completion, the conformation with the most favorable binding energy and the highest frequency of recurrent binding poses was selected as the output. The results were then imported into PyMOL 3.1 and Discovery Studio 2019 for visualization and analysis.

The rigid docking experiment between BDNF (UniProt ID P21237) and TLR4 (UniProt ID Q9QUK6) proteins was performed using the GRAMM platform. Protein structures were sourced from the UniProtKB database, and calculations were initiated using the platform's default PPI docking parameters. Upon completion of docking, the binding free energy was calculated with PDBePISA, and visualization analysis was conducted using PyMOL 3.1.

Animals

Male BDNF conditional knockout (cKO) mice were generously provided by the laboratory of Professor Zheyu Chen, Department of Neurobiology, Shandong University. Male SPF grade C57BL/6 mice (8 weeks old) were purchased from Liaoning Changsheng Biotechnology Co., Ltd. All animals were housed under controlled conditions with a constant temperature of 20 ± 2°C, relative humidity of 50 ± 5%, and a 12-

hour light/dark cycle, with ad libitum access to food and water. All experimental procedures involving animals were conducted in accordance with the guidelines approved by the Institutional Animal Care and Use Committee.

Cell Cultivation

SH-SY5Y cells were purchased from Wuhan Zishan Biological Co., Ltd. Cells were maintained in DMEM supplemented with 10% fetal bovine serum (FBS) under standard culture conditions of 37 °C, 5% CO_2, and saturated humidity. To induce neurotoxicity in vitro, cells were exposed to 0.5 mM MPP^+ (Macklin, batch number:C17441450) in the presence or absence of various concentrations of GS or individual GS (Re, Rf, Rg2, Rc, Ro) for 24 h. Cell viability was assessed using the CCK-8 assay: after treatment, CCK-8 solution (BIOSS, batch number:BE05068677) was added to each well and incubated at 37 °C for 1 h, followed by measurement of absorbance at 450 nm using a microplate reader.

Animal Grouping and Behavior Assessment

Following a 7-day acclimatization period, mice were intraperitoneally injected with MPTP at a dose of 25 mg/kg daily for 7 consecutive days, while the control group received an equivalent volume of normal saline. Successful model establishment was determined based on significant behavioral changes observed after MPTP administration compared to baseline. Successfully modeled wildtype mice were randomly assigned to the following groups: MPTP group, positive control (P.C.) group (Carbidopa and Levodopa Sustained Release Tablets, 50 mg/kg[32]), GS high-, medium-, and low-dose groups (100, 50, and 25 mg/kg, respectively), and GsRe group (40 mg/kg). BDNF cKO mice were randomly divided into the MPTP and GsRe (40 mg/kg) groups. All treatments were administered via oral gavage once daily for 21 consecutive days. The control and model groups received an equivalent volume of normal saline. Drug dosing in the treatment groups was based on body weight, with the vehicle control group receiving saline at a volume equivalent to the 50 mg/kg dose.

Pole Test: The pole climbing test is commonly employed to evaluate muscle strength and motor coordination in small rodents. A wooden rod (30 cm in length, 2 cm in diameter) is vertically fixed inside a rectangular plastic chamber, with two turns of gauze wrapped around its surface to enhance grip friction. The mouse is gently held by the tail and positioned head down so that its forepaws contact the top of the rod to initiate the test; timing begins upon release and ends when the forepaws touch the base of the chamber. Each mouse undergoes three trials, with a 20-minute inter trial interval to minimize fatigue and habituation. The average of the three measurements is calculated and used as the final experimental value.

Hanging Rope Test: A metal wire approximately 40 cm in length was horizontally fixed at a height of 30 cm above the ground. Mice were placed on the wire and allowed to grasp its center with their forepaws. Motor performance was evaluated using a standardized scoring system: (1) Hindlimb grip latency: mice that grasped the wire within 0–4 s, 5–9 s, 10–19 s, 20–39 s, and ≥40 s received scores of 5, 4, 3, 2, and 1, respectively; (2) Time to reach either end of the wire: completion within 0–39 s, 40–59 s, 60–99 s, 100–

129 s, and ≥130 s was scored as 5, 4, 3, 2, and 1, respectively; (3) Latency to fall: mice that did not fall, fell after ≥120 s, between 60–119 s, 20–59 s, or before 20 s were assigned scores of 5, 4, 3, 2, and 1, respectively. All animals underwent five training trials prior to testing, followed by three formal test trials. The total clinical score for each mouse was calculated as the sum of the scores from all three categories.

Morris Water Maze Test: The Morris water maze consists of a circular pool 120 cm in diameter and 50 cm in height, filled with water and equipped with a hidden escape platform 10 cm in diameter, positioned 1 cm below the water surface. Water temperature was maintained at (24 ± 1) °C using a heating system. The platform was fixed in the center of one quadrant and remained submerged and invisible throughout the experiment. Mice were released from the opposite quadrant relative to the platform location. The escape latency, the time taken for the mouse to locate and mount the submerged platform, was recorded as the primary measure of spatial learning and memory performance. If a mouse failed to find the platform within 60 s, the trial was terminated, and an escape latency of 60 s was assigned.

Open Field Test: The open field test is widely used to evaluate spontaneous locomotor activity and anxiety like behaviors in mice, providing an indirect measure of motor impairment in PD models. The apparatus consists of a square arena (40 × 40 × 30 cm) divided into central and peripheral zones. Each mouse is individually placed in the center of the arena, and its movement trajectory is recorded over a 5-minute period using an automated tracking system.

Gait Analysis: The forepaws and hind paws of mice were marked with red and blue ink, respectively. Each mouse was then gently placed at one end of a narrow runway (90 cm × 4.5 cm × 15 cm) lined with white paper and encouraged to traverse to the opposite end, producing a continuous sequence of footprints. Stride length was determined as the average distance between consecutive left paw prints.

Animal Materials and Processing

Tissue collection was performed the day after completion of behavioral testing. Mice were subjected to retro orbital blood collection under isoflurane inhalation anesthesia following a 12-hour fasting period without food or water. After blood sampling, mice were deeply anesthetized and transcranial perfused: for a subset of animals, perfusion was carried out with phosphate buffered saline (PBS) followed by 4% paraformaldehyde (PFA); brains were then dissected and post fixed in 4% PFA at 4 °C for histological analysis. In the remaining mice, transcranial perfusion was performed with PBS only, after which brains were rapidly removed. The striatum and substantia nigra were micro dissected on ice, immediately frozen in liquid nitrogen, and stored at -80 °C for subsequent biochemical assays.

Nissl's Staining

Mouse brain tissue sections were stained with toluidine blue and subsequently dehydrated through a graded ethanol series: 95% ethanol for 5 minutes, followed by 100% ethanol for 10 minutes. The sections were then cleared in xylene for 10 minutes and cover slipped using a permanent mounting medium.

ELISA Assay

The levels of pro-inflammatory and anti-inflammatory cytokines, including TNF-α, IL-1β, TGF-β, and IL-10, in brain tissue were quantified using enzyme linked immunosorbent assay (ELISA). All ELISA kits were commercially obtained from Shanghai Youxuan Biotechnology Co., Ltd., and assays were performed according to the manufacturer's instructions.

Proteomics Analysis

Substantia nigra (SNpc) brain tissues were collected from wild-type and BDNF cKO mice in the MPTP and MPTP + Re groups (n = 3 per group) and immediately flash frozen in liquid nitrogen. Proteomic analysis was conducted by Jingjie Biotechnology Co., Ltd. (Hangzhou, China). In brief, proteins were extracted from tissue samples, and protein concentrations were determined using the BCA assay. Equal amounts of protein were subjected to tryptic digestion. Resulting peptides were dissolved in mobile phase A for liquid chromatography and separated on a Vanquish Neo UPLC system. The eluted peptides were subsequently ionized via a nano electrospray ion source and analyzed by data-independent acquisition (DIA) on a timsTOF HT mass spectrometer. Raw DIA data were processed using DIA-NN (v.1.8), with tandem mass spectra searched against the Mus_musculus_10090_SP_20241202.fasta database (17,236 entries) concatenated with a reverse decoy database. Trypsin/P was designated as the proteolytic enzyme, allowing up to one missed cleavage site. Fixed modifications included N-terminal methionine excision and carbamidomethylating of cysteine residues. False discovery rates (FDR) at both peptide and protein levels were controlled at 1%. Protein abundances, expressed as normalized intensity (I), were centrally transformed to derive relative quantification values (R) across samples for comparative analysis. Proteins exhibiting a fold change>1.2 and an adjusted p-value<0.05 were considered significantly differentially expressed. Bioinformatics analyses, including GO functional annotation and KEGG pathway enrichment, were performed using the Jingjie Cloud Platform.

Immunofluorescent Staining

Paraffin embedded sections of the tissues of the SNpc were deparaffinized and rehydrated through a graded alcohol series to distilled water, followed by antigen retrieval via heat induced epitope retrieval (HIER). A hydrophobic barrier was drawn around the tissue sections using a PAP pen. Endogenous peroxidase activity was quenched with 3% hydrogen peroxide, and nonspecific binding sites were blocked with normal serum. Prepared primary antibodies, including anti-TH (Proteintech, 25859-1-AP, 1:4000), anti-DAT (Proteintech, 22524-1-AP, 1:1000), anti-Iba-1 (Servicebio, GB113502, 1:5000), anti-CD86 (Servicebio, GB150054, 1:2500), anti-CD206 (Servicebio, GB115273, 1:4000), and anti-NF-κB (Servicebio, GB11997, 1:1500), were applied and incubated overnight at 4°C. This was followed by a 1-hour incubation with corresponding secondary antibodies. Tyramide signal amplification (TSA) reagent was added within the marked area and incubated in the dark for 10 minutes. Subsequently, microwave assisted stripping was performed to remove bound antibodies while preserving tissue integrity. After blocking, the second primary antibody was applied, followed by its respective HRP labeled secondary antibody and TSA development. Nuclei were counterstained with DAPI for 10 minutes. Fluorescence

images were captured using a Nikon ECLIPSE C1 fluorescence microscope (Nikon, Tokyo, Japan). Fluorescence intensity for each region of interest was quantified using ImageJ software.

Immunoblotting Analysis

Mouse striatal tissue was homogenized in RIPA lysis buffer supplemented with protease and phosphatase inhibitors. Protein concentrations were determined using a BCA assay kit, and equal amounts of protein (20 μg per sample) were loaded onto gels. Proteins were separated by Tris-HCl polyacrylamide gel electrophoresis (PAGE) and subsequently transferred to PVDF membranes. After blocking with 5% skimmed milk, the membrane was incubated overnight at 4 °C (approximately 16 hours) with anti-α-Synuclein (Selleck, F0564,1:1000), anti-TH (Proteintech, 25859-1-AP,1:1000), anti-DAT (Proteintech, 22524-1-AP,1:1000), anti-BDNF (Proteintech, 28205-1-AP,1:1000), anti-TrkB (Proteintech, 13129-1-AP,1:1000), anti-BAX (Proteintech, 50599-2-Ig,1:1000), anti-Caspase 3/P17/P19 (Proteintech, 19677-1-AP,1:1000), anti-WDFY1 (Proteintech, 13960-1-AP,1:1000), anti-TRIF/TICAM1 (ABclonal, A13605,1:5000), anti-STAT1 (ABclonal, A12075,1:1000), anti-Bcl-2 (ABclonal, A0208,1:2000), anti-phospho-NF-κB (S529) (HUABIO, ET1604-27,1:1000), anti-NF-κB (HUABIO, ET1603-12,1:1000) or anti-TLR4 (Zenbio, 505258,1:500) antibodies. Followed by incubation with horseradish peroxidase (HRP) conjugated goat anti-rabbit IgG secondary antibody for 30 minutes at room temperature. Immunoreactive bands were visualized using the Tanon 5200 chemiluminescent imaging system. Band intensities were quantified by measuring integrated pixel density using ImageJ software, and data were subjected to optical density analysis.

Co-Immunoprecipitation (Co-IP)

The tissues were lysed using IP lysis buffer containing protease inhibitors, with the lysis process carried out on ice for 30 minutes. The lysate was centrifuged at 11,000 g for 15 minutes at 4°C to isolate the supernatant. Protein concentration was determined using a BCA assay kit and adjusted to 1000 mg/ml. A 50 μL aliquot of the supernatant was collected as the input sample. To the remaining lysate, 20 μL of pre-balanced Protein A/G magnetic beads were added, followed by gentle agitation and incubation at 4°C for 1 hour. The precleared lysate was equally divided into two portions. BDNF antibody (Santa Cruz, sc-65514) and mouse IgG antibody (Beyotime, A7028) were added at a ratio of 2 μg antibody per 500 μg of protein, respectively, and incubated overnight at 4°C. Subsequently, 30 μL of Protein A/G magnetic beads were added to each sample and incubated at 4°C for 2 hours. Finally, the beads were washed six times with cell lysis buffer, resuspended in 20–30 μL of 1× loading buffer, and boiled at 100°C for 10 minutes. The magnetic beads were separated magnetically, and the supernatant containing the target antigen was collected for further western blot analysis.

Statistics Analysis

Statistical analysis was performed using GraphPad Prism 9.5 software. All data are expressed as mean ± standard deviation (Mean ± S.D.). Student’s two tailed t-test was employed for two group comparisons.

For multi-group comparisons, one-way ANOVA with LSD post hoc testing was used where appropriate. A P value < 0.05 was considered statistically significant.

Results

Chemical Profiling and Network Pharmacology Investigation of GS

Qualitative analysis was performed using UHPLC-Q-Orbitrap-MS/MS, enabling precise identification of 11 ginsenoside components through comparison of retention times and fragment ion spectrum with reference standards and published data (Supplementary Fig 1). Subsequent quantitative analysis of major constituents was carried out via UPLC, revealing the following contents: ginsenoside Rg1 (3.00%), Re (11.78%), Rf (2.34%), Rg2 (0.98%), Rb1 (21.28%), Ro (11.41%), Rc (0.17%), Rb2 (10.73%), and Rd (8.74%) (Table 1).

To elucidate the potential mechanisms underlying the therapeutic effects of GS in PD, a network pharmacology approach was employed. Through systematic database mining, 246 potential targets associated with GS active components and 1,275 PD related targets were identified. A total of 54 overlapping targets were recognized as candidate therapeutic targets for GS in PD (Fig 1A). Functional enrichment analysis using Gene Ontology (GO) and Kyoto Encyclopedia of Genes and Genomes (KEGG) pathways were conducted to characterize the biological processes and signaling pathways implicated in GS mediated PD intervention. KEGG analysis revealed 105 significantly enriched signaling pathways ($P < 0.01$); the top 20 PD relevant pathways were selected based on statistical significance and visualized using a Chord diagram generated by Sangerbox 3.0 to map the interplay between key targets and pathways (Fig 1B). The results highlighted neurotrophic factor signaling, TLR signaling and NF-κB signaling as central pathways modulated by GS in PD (Fig 1C). Dysregulation of neurotrophic factor signaling has been linked to dopaminergic neuron degeneration and may contribute to synaptic dysfunction and neuronal apoptosis under neuroinflammatory conditions, suggesting its pivotal role in PD pathogenesis. Notably, the TLR4/NF-κB signaling axis, recognized as a core regulator of innate immunity and inflammatory responses, has been shown to be aberrantly activated in PD and closely associated with progressive dopaminergic neuron loss[33]. GO enrichment further indicated that GS targets biological processes including lipopolysaccharide mediated signaling, dopaminergic synaptic transmission, and astrocyte activation (Fig 1D).

To integrate these findings, a "component/target/pathway/disease" network was constructed using Cytoscape, incorporating chemical components, shared targets, and the top 20 KEGG pathways, thereby providing a comprehensive visualization of the potential therapeutic mechanism of GS in PD (Fig 1E). Topological analysis of the network identified GsRe, Rf, Rg2, Rc and Ro as hub components with high connectivity, suggesting their critical roles in mediating therapeutic effects. These compounds are predicted to act on key targets such as BDNF and modulate crucial pathways including neurotrophic signaling. Supporting evidence indicates that GsRe activates the BDNF/TrkB/ERK/CREB pathway, conferring neuroprotective and antidepressant effects[30]. Ginsenoside Rg3 alleviates brain damage

caused by chlorpyrifos exposure by targeting and regulating the microbial/gut/brain axis[34]. Rc exerts antifibrotic effects by suppressing the TLR4 signaling pathway and inactivating hepatic stellate cells[35]. Collectively, these findings strongly suggest that the therapeutic potential of GS in PD may be mediated through modulation of BDNF dependent neurotrophic support and suppression of TLR4 driven neuroinflammation.

GS Ameliorate Motor Dysfunction and Neuronal Injury in MPTP Induced PD Mouse Models

A schematic diagram of animal experimental design is provided (Fig. 2A). The body weight of the mice was monitored weekly during the experimental period (Fig 2B). Following MPTP modeling, the mice exhibited a significant decrease in body weight. After the completion of modeling, their body weight gradually recovered, showing an overall upward trend. Mice in the GS administration group exhibited a faster recovery rate in body weight compared to those in the MPTP group.

To systematically evaluate the therapeutic effects of GS on motor dysfunction in MPTP induced PD mouse models, this study employed three behavioral assays, Morris's water maze (MWM), pole climbing test, and hanging rope test, to comprehensively assess motor performance across multiple domains, including spatial learning and memory, limb coordination, muscle strength, and balance control. In the MWM task, MPTP treated mice exhibited significantly prolonged escape latency and increased total swimming path length, indicating impairments in spatial learning, memory acquisition, and locomotor precision. Notably, GS treatment markedly reduced both parameters (Fig 2C-2E), suggesting improved cognitive motor integration.

In the pole climbing test, GS treated mice showed a significant reduction in descent time compared to the MPTP group (Fig 2G). Similarly, in the hanging rope test, GS administration led to a significant increase in composite scores (Fig 2F), reflecting enhanced forelimb muscle strength and postural stability. These behavioral improvements indicate that GS ameliorates MPTP induced motor deficits.

Nissl staining revealed a significant loss of neurons in the tissues of the SNpc of MPTP treated mice, characterized by shrunken cell bodies, pale and sparse Nissl bodies, and nuclear pyknosis. GS treatment attenuated these histopathological changes to varying degrees, preserving neuronal integrity (Fig 2H-2I).

Immunohistochemical analysis demonstrated a marked reduction in TH positive neurons in the substantia nigra of MPTP mice, along with fragmented or absent neurites, indicative of severe dopaminergic neuron degeneration. Both the positive control and GS treated groups exhibited increased survival of TH positive neurons, with the high dose GS group showing the most pronounced effect (Fig 2J-2K). This indicates a dose dependent neuroprotective action of GS on nigral dopaminergic neurons.

In the striatum, MPTP exposure upregulated α-synuclein expression and downregulated TH and DAT protein levels, changes that were effectively reversed by GS treatment (Fig 2L). These findings demonstrate that GS mitigates MPTP induced dopaminergic neurodegeneration, suppresses

pathological α-syn accumulation, and restores TH expression, thereby exerting robust neuroprotection within the nigrostriatal pathway.

Western blot analysis further indicated that the neuroprotective effects of GS may be mediated through activation of the BDNF/TrkB signaling pathway, as GS treatment significantly restored the MPTP induced downregulation of both BDNF and TrkB protein expression (Fig 2M-2O).

GS attenuate MPTP Induced Neuroinflammation and Neuronal Apoptosis Following with Activation of the TLR4/NF-κB Signaling Pathway

Compared with the MPTP group, both the P.C. group and total saponin treatment groups significantly attenuated MPTP induced elevations in pro-inflammatory cytokines TNF-α and IL-1β, while concurrently increasing the levels of anti-inflammatory cytokines TGF-β and IL-10 (Fig 3A–3D). Notably, the anti-inflammatory effect of total saponins exhibited a clear dose dependent pattern.

TLR4 activation upon recognition of pathogen or damage associated molecular patterns triggers the MyD88 dependent phosphorylation of NF-κB, leading to the transcription of pro-inflammatory mediators such as TNF-α and IL-1β, thereby constituting a central mechanism in the initiation and amplification of neuroinflammation[36]. To investigate whether GS modulate this pathway, we assessed the expression of TLR4, NF-κB, and p-NF-κB by Western blot. The data revealed that total ginsenoside treatment, particularly at medium and high doses, markedly suppressed MPTP-induced upregulation of TLR4 and p-NF-κB protein expression (Fig. 3F-3G).

Given that nuclear translocation of NF-κB is a critical step in transducing TLR4 signaling from the membrane to the nucleus and activating inflammatory gene expression [37], we further evaluated NF-κB localization using immunofluorescence (Fig. 3E). In the control group, NF-κB was predominantly localized in cytoplasm with minimal nuclear signal; in contrast, the MPTP group exhibited pronounced nuclear translocation, which was substantially reduced following GS treatment, as evidenced by a decreased nuclear to cytoplasmic ratio.

Collectively, these findings indicate that GS ameliorate PD like pathology by suppressing pro-inflammatory cytokine production and inhibiting TLR4/NF-κB pathway activation.

Moreover, accumulating evidence suggests that hyperactivation of the TLR4/NF-κB axis not only drives robust neuroinflammatory responses but also promotes dopaminergic neuronal apoptosis through regulation of downstream apoptotic molecules[38]. To assess the protective effects of GS against MPTP induced neuronal apoptosis, we analyzed the expression of key apoptosis-related proteins by Western blot (Fig. 3H-3I). Our results showed that GS treatment effectively reversed the dysregulation of apoptotic markers induced by MPTP, with a response that was consistently dose dependent.

GsRe Targets BDNF to Enhance Dopamine Levels, Suggesting A Potential Mechanism for Its Neuroprotective Effects

To elucidate the pharmacological basis underlying its therapeutic effects, the researchers first determined the optimal modeling concentration of MPP^+ and established the safe concentration range of individual ginsenoside monomers (Supplementary Fig 2A-2B). Subsequently, the CCK-8 assay was employed to assess their protective effects in an SH-SY5Y neuronal cell injury model induced by MPP^+ (Supplementary Fig 2C). Among the five tested monomers, GsRe exhibited the most potent neuroprotective activity, demonstrating the greatest efficacy in reversing MPP^+ induced reduction in cell viability (Fig 4A).

Molecular docking simulations indicated a potential interaction between GsRe and the neurotrophic factor BDNF (Fig 4B), the docking binding energy was determined to be -7.4 kJ/mol. This finding was further supported by Western blot analysis, which revealed that GsRe treatment significantly upregulated the protein expression of both BDNF and its receptor TrkB (Fig 4C), suggesting activation of the BDNF/TrkB signaling pathway as a likely mechanism of action.

In vivo experiments demonstrated that GsRe administration markedly increased dopamine levels in the serum, SNpc and striatum of PD model mice (Fig 4D–4F). Furthermore, pharmacokinetic analysis confirmed the presence of GsRe in systemic circulation and its distribution to critical brain regions, including the substantia nigra and striatum (Fig 4G–4I). The total ion chromatograms of GsRe and DA are shown (Supplementary Fig. 3). Taken together, these results indicate that GsRe exerts neuroprotective effects by targeting BDNF signaling and restoring dopaminergic neurotransmission.

GsRe Ameliorates Motor Deficits in PD Model Mice and Attenuates the Degeneration of Dopaminergic Neurons

To investigate the essential role of the BDNF pathway in mediating the neuroprotective effects of GsRe, the researchers evaluated the impact of GsRe treatment on BDNF cKO mice.

Both BDNF cKO and WT model mice exhibited pronounced motor dysfunction. Notably, BDNF cKO mice displayed significantly worse performance across multiple behavioral tests compared to WT model mice, indicating that BDNF deficiency exacerbates motor impairments. GsRe administration markedly improved motor function in both BDNF cKO and WT PD mice.

In the open field test, GsRe treated BDNF cKO and WT mice showed a significant increase in total travel distance relative to their respective vehicle treated model groups (Fig 5A). Gait analysis revealed that GsRe treatment significantly increased stride length (Fig 5B). Additionally, treated mice exhibited a significant reduction in pole climbing time (Fig 5C) and a notable prolongation of hanging time (Fig 5D), demonstrating substantial recovery in motor coordination and endurance. Collectively, these data indicate that GsRe effectively ameliorates MPTP induced motor deficits.

Immunohistochemical analysis of TH in the substantia nigra demonstrated that GsRe intervention attenuated dopaminergic neuronal loss (Fig 5E). Furthermore, immunofluorescence staining of TH and DAT in the substantia nigra and striatum revealed that GsRe significantly enhanced the expression of

dopaminergic markers and reduced dendritic fragmentation and atrophy (Fig 5F–5J). Western blot analysis confirmed that GsRe treatment significantly suppressed the abnormal aggregation of α-syn while upregulating protein levels of TH and DAT (Fig 5K–5M).

These findings demonstrate that GsRe not only improves motor behavior in MPTP induced PD model mice but also exerts robust neuroprotection by preserving dopaminergic neuron integrity and promoting neuron survival. Importantly, the neuroprotective efficacy of GsRe was substantially diminished in BDNF cKO mice, strongly suggesting that its beneficial effects are mediated, at least in part, through the BDNF signaling pathway.

BDNF Deficiency Exacerbates the Pathological Progression of PD and Intensifies Neuroinflammatory Responses in the Mouse Brain

Analysis of the GSE49036 dataset from the Gene Expression Omnibus (GEO) database revealed a significant downregulation of BDNF in the brains of PD patients (Supplementary Fig 4C), which was negatively correlated with the extent of neuronal degeneration[16]. To investigate the role of BDNF deficiency in PD pathogenesis, a murine model of PD was established using BDNF cKO and WT mice. Dopaminergic neurons were identified and quantified by immunohistochemical staining for TH in the SNpc. Both WT and BDNF cKO mice exhibited a significant reduction in the number of TH positive neurons in the SNpc compared to controls, with a more pronounced loss observed in the BDNF cKO group (Fig 6A-6B). Western blot analysis further confirmed a marked decrease in TH protein expression, a key rate limiting enzyme in dopamine synthesis, in the brains of BDNF cKO mice, accompanied by a significant upregulation of α-syn (Fig 6C-6D). Consistent with these findings, ELISA measurements revealed a substantial reduction in striatal dopamine levels in BDNF cKO mice compared to controls (Fig 6E).

Neurological dysfunction was further reflected in motor behavioral deficits. Motor coordination and muscle strength were assessed using the hanging wire test and pole test. In the hanging wire test, MPTP treated mice displayed significantly shorter latency to fall, indicative of reduced grip strength and impaired neuromuscular endurance. This deficit was exacerbated in BDNF cKO mice, which showed significantly lower composite scores than control animals (Fig 6F), suggesting greater impairment in forelimb strength and overall motor balance. Similarly, in the pole test, MPTP treated mice required significantly longer times to descend from the top to the base of the pole, with BDNF cKO mice exhibiting even more severe delays (Fig 6G), reflecting compromised limb coordination and bradykinesia. These behavioral impairments recapitulate core motor symptoms of PD, including akinesia, muscle weakness and postural instability.

To examine the contribution of BDNF deficiency to neuroinflammation, levels of pro-inflammatory cytokines TNF-α and IL-1β were measured in brain tissue by ELISA. As diagrams illustrated (Fig 6H-6I), BDNF cKO mice exhibited significantly elevated levels of both TNF-α and IL-1β, indicating robust activation of microglia and a heightened neuroinflammatory state. This chronic inflammatory response may serve as a critical mechanism underlying the accelerated degeneration of dopaminergic neurons.

Collectively, these results demonstrate that BDNF deficiency exacerbates MPTP induced Parkinsonian phenotypes, including dopaminergic neuron loss, neurotransmitter depletion, motor dysfunction, and neuroinflammation, highlighting its pivotal role in modulating disease progression.

Proteomic analysis reveals BDNF deficiency mediated hyperactivation of the Toll like receptor signaling pathway

To elucidate the molecular mechanisms underlying BDNF deficiency induced exacerbation of dopaminergic neuron damage and to investigate the therapeutic effects of GsRe, a label free quantitative proteomic analysis was performed on SNpc tissues from WT and BDNF cKO PD model mice.

The distribution of peptide lengths and quantities demonstrates that the data meets the quality control criteria (Supplementary Fig 5A-5B). Principal component analysis revealed that BDNF deficiency significantly altered the global protein expression profile (Supplementary Fig 5C,5E). Volcano plot analysis showed that the fold changes of differentially expressed proteins were relatively concentrated and conformed to a normal distribution (Fig 6J). Comparative analysis between the BDNF cKO_PD and WT_PD groups identified 175 differentially expressed proteins (DEPs), including 103 upregulated and 72 downregulated proteins (Supplementary Fig 5D).

KEGG pathway enrichment analysis demonstrated significant activation of immune and inflammation related pathways in the BDNF cKO_PD group, including antigen processing and presentation, TLR signaling, Th17 cell differentiation and necroptosis (Fig 6K). GO term enrichment further revealed prominent involvement of biological processes such as positive regulation of neurotransmitter uptake, cellular response to IL-β and antigen binding (Supplementary Fig 5F), collectively suggesting that BDNF deficiency triggers aberrant activation of innate immune and inflammatory responses. In particular, the TLR signaling pathway was significantly regulated in the BDNF cKO group, indicating a close association between the TLR signaling pathway and BDNF.

Proteomic Analysis of GsRe Exerts Neuroprotective Effects by Suppressing BDNF Deficiency Mediated Hyperactivation of the TLR Signaling Pathway

To determine whether GsRe exerts its neuroprotective effects through modulation of the interaction between BDNF and the TLR pathway, a comprehensive analysis was conducted on the expression levels of key regulatory proteins. Western blot analysis revealed that, compared with the model group, GsRe intervention significantly upregulated BDNF protein expression in the substantia nigra while downregulating TLR4 levels, suggesting an inverse relationship between these two molecules (Fig 7D).

To further investigate the underlying molecular mechanism, Co-IP assays were performed to assess the physical interactions between BDNF and critical components of the TLR4 pathway. The results showed that BDNF could specifically bind to TLR4, and GsRe administration enhanced the binding affinity between BDNF and TLR4 (Fig 7D). Molecular docking reveals that the amino acid residues THR-39, GLU-105, and CYS-241 of the BDNF protein exhibit specific interactions with the amino acid residues THR-

624, LYS-595, and LYS-56 of the TLR4 protein (Fig 7E). The binding energy is -20.5 kcal/mol, indicating that the two target proteins can form a stable interaction system on the surface. It suggests that GsRe inhibits the activity of the TLR signaling pathway by enhancing the inhibitory effect of BDNF on TLR4.

Proteomic analysis was performed to detect changes in the protein profile following GsRe intervention, which identified 117 differentially expressed proteins in the GsRe treated group (BDNF cKO_Re vs. BDNF cKO_PD), comprising 51 upregulated and 66 downregulated proteins (Supplementary Fig 5D). Further overlap analysis showed that 8 proteins previously downregulated in the BDNF cKO_PD group were restored toward normal levels after GsRe treatment, while 14 upregulated proteins exhibited reversed expression patterns upon intervention (Fig 7A). Heatmap analysis of overlapping differentially expressed proteins identified in the Venn diagram (Fig 7B).

Upon GsRe treatment, KEGG analysis revealed that the antigen processing and presentation pathway, Toll-like receptor signaling pathway, and Th17/Th1/Th2 cell differentiation pathway were downregulated (Fig 7C). Further GO analysis showed significant enrichment of terms including positive regulation of TRAIL production, T cell mediated immune regulation, TAP binding, and MHC protein complex formation (Supplementary Fig 5G), suggesting that the body's inflammatory and immune responses were alleviated.

Notably, the TLR signaling pathway was markedly upregulated in BDNF cKO_PD mice. Volcano plot analysis identified two key proteins in this pathway, WDFY1 and STAT1, which were significantly downregulated following GsRe intervention (Fig 7G). This explains why GsRe can still inhibit the aberrant activation of the TLR signaling pathway under the condition of BDNF deficiency. WDFY1 is known to function as a critical adaptor protein in the TLR4/TRIF axis, facilitating TRIF recruitment to TLR4 and thereby promoting downstream NF-κB and STAT1 activation[39]. GsRe intervention may inhibit the overall activity of the TLR signaling pathway by reversing the aberrant expression of these two proteins (Fig 7H).

We further analyzed the changes in key molecules in the TLR4 signaling pathway. Western blot analysis results showed that GsRe intervention could significantly reduce the expression levels of TLR4 and its downstream adaptor TRIF and effectively inhibit the phosphorylation of NF-κB (p-NF-κB) as well as the protein expression of STAT1 (Fig 7F).

These findings indicate that BDNF deficiency drives pathological overactivation of neuroinflammatory signaling, particularly through the TLR pathway, and that GsRe exerts neuroprotective effects, at least in part attenuating this maladaptive immune response.

GsRe Inhibits TLR4 Mediated Neuroinflammation, Microglial Polarization and Neuronal Apoptosis

To explore the downstream consequences of GsRe mediated regulation of the BDNF/TLR4 axis, the study systematically evaluated neuronal apoptosis and microglia driven neuroinflammation. Studies have shown that microglia, the primary immune cells in the central nervous system, are normally in a

resting state. Damage associated molecular patterns such as pathological α-syn activate microglia via the TLR pathway[40], leading to their polarization toward the proinflammatory phenotype (M1 type) and the release of proinflammatory cytokines including TNF-α and IL-1β[41].

Immunofluorescence staining was employed to evaluate microglial phenotypes (Fig 8A). GsRe treatment significantly reduced fluorescence intensity of CD86, a marker of M1 microglia, while increasing expression of CD206, an M2 phenotype marker, leading to a marked decrease in the CD86/CD206 ratio (Fig 8B). Additionally, the signal intensity of Iba-1, a general marker of microglial activation, was attenuated (Fig 8C).

ELISA was used to detect the expression levels of inflammatory factors in brain tissues. The results showed that after GsRe intervention, the levels of pro-inflammatory factors IL-1β and TNF-α in brain tissues were significantly decreased, while the levels of anti-inflammatory factors TGF-β and IL-10 were significantly increased (Fig 8D-8G). These results indicate that GsRe effectively shifts microglia from a pro-inflammatory M1 state toward an anti-inflammatory M2 phenotype, thereby ameliorating the neuroinflammatory milieu.

GsRe treatment markedly increased the anti-apoptotic protein BCL-2, decreased levels of the pro-apoptotic protein Bax and inhibited cleavage of Caspase-3 (Fig 8H-8I). These changes align with previous reports showing that hyperactivation of the TLR4/NF-κB pathway can alter the BCL-2/Bax ratio and promote caspase-3 activation[42]. By effectively inhibiting the TRIF/NF-κB signaling axis downstream of TLR4, GsRe blocked the TLR4 mediated apoptotic signaling, which may represent a key mechanism underlying its anti-apoptotic effects.

Collectively, these findings demonstrate that GsRe exerts neuroprotection by enhancing the interaction between BDNF and TLR4, leading to suppression of the downstream TLR4/TRIF/NF-κB signaling pathway. This inhibition subsequently reverses microglial M1 polarization, alleviates neuroinflammation, and prevents neuronal apoptosis. These data support a central mechanism by which GsRe modulates neuroimmune crosstalk to confer protection in PD models.

Discussion

This study systematically investigated the neuroprotective effects and underlying mechanisms of GS and their major active constituent, GsRe, in MPTP induced PD. First, the chemical composition of GS was comprehensively characterized using UHPLC-Q-Orbitrap-MS/MS, followed by network pharmacology analysis to predict potential molecular mechanisms involved in PD. The results indicated that these mechanisms are closely associated with TLR4/NF-κB pathway mediated neuroinflammation and apoptosis, as well as BDNF signaling regulation. In an in vivo mouse model of MPTP induced PD, treatment with GS significantly ameliorated motor deficits, protected dopaminergic neurons, and reduced neuroinflammatory responses, as demonstrated through behavioral assessments, histopathological staining, and detection of key proteins. To identify the primary bioactive component

responsible for these effects, a CCK-8 based screening assay revealed that GsRe is the core neuroprotective agent within GS. Notably, BDNF deficiency was shown to exacerbate both neuropathological progression and central inflammatory responses, highlighting its critical role in PD pathogenesis. Further mechanistic investigations demonstrated that GsRe not only restored dopamine levels and prevented dopaminergic neuronal loss but also specifically suppressed overactivation of the TLR4/NF-κB pathway by enhancing the interaction between BDNF and TLR4. Proteomic profiling corroborated these findings, confirming that GsRe modulates the BDNF regulated TLR signaling cascade, thereby inhibiting neuroinflammation and apoptosis. Collectively, these results provide a systematic elucidation of the molecular mechanism by which GsRe, as a key active constituent of GS, exerts neuroprotection via regulation of the BDNF/TLR4 axis, offering a strong theoretical foundation for the development of natural product based therapeutic strategies against PD.

Complex mixture of bioactive saponins in GS that exhibit multitarget neuroprotective effects in the MPTP induced PD model. These compounds can modulate multiple core pathological processes in PD pathogenesis, including mitochondrial dysfunction Ginsenoside Rg3 Restores Mitochondrial Cardiolipin Homeostasis vi, neuroinflammation[43], impaired autophagic degradation[44], and deficient neurotrophic support[45]. Among the various constituents of GS, GsRe emerges as a particularly promising candidate due to its potent neuroprotective properties. The protective efficacy of GsRe has been consistently demonstrated in animal models of PD induced by neurotoxins such as rotenone and MPTP[46-48]. In this study, we found that GsRe effectively penetrates critical brain regions, including the SNpc and striatum, thereby exerting direct therapeutic actions on key neuropathological sites. Under normal physiological conditions, GsRe levels in brain tissue are relatively low[49]. However, in the context of PD pathology, increased blood brain barrier permeability enhances the cerebral distribution of GsRe, facilitating its accumulation at lesion sites.

Accumulating evidence demonstrates that the immune system and chronic neuroinflammation play a central role in the pathogenesis of PD[50]. Within the innate immune response, TLR4 has emerged as a critical mediator of neuroinflammatory signaling and disease progression[51, 52]. In PD patients, TLR4 expression is upregulated in peripheral blood mononuclear cells and positively correlates with circulating TNF-α levels[53]. During PD pathogenesis, misfolded α-syn forms oligomers and fibrillar aggregates[54], which are recognized by TLR4 expressed on microglia and neurons, thereby initiating innate immune activation[55]. Activation of TLR4 on microglia induces NF-κB signaling via MyD88 or TRIF dependent pathways[56]. This NF-κB activation suppresses both autophagy and the ubiquitin proteasome system, impairing α-syn clearance and consequently exacerbating neuropathology[57]. Furthermore, NF-κB drives the polarization of microglia toward a pro-inflammatory M1 phenotype, leading to the release of inflammatory cytokines such as TNF-α and IL-1β[58]. These mediators not only directly damage dopaminergic neurons but also induce oxidative stress and mitochondrial dysfunction, ultimately activating the caspase cascade and promoting neuronal apoptosis[59].

BDNF plays a critical role in the pathogenesis of PD. In this study, BDNF deficiency was shown to exacerbate MPTP induced PD pathology, as evidenced by increased α-syn levels, reduced TH expression, decreased striatal DA concentrations, and worsened motor dysfunction. Notably, while BDNF deficiency does not directly alter TH protein expression under baseline conditions, BDNF deficient mice exhibit lower striatal DA level, a finding consistent with previous reports, potentially attributable to age dependent differences in dopamine uptake capacity[60]. Behavioral assessments revealed significantly impaired motor performance in BDNF deficient mice. Rantamäki et al. have further demonstrated that BDNF deficiency impairs spatial learning, spontaneous exploratory behavior, and motor coordination in both male and female mice at 12 months of age, with obesity potentially exacerbating these deficits[61]. This motor dysregulation may be linked to a marked reduction in glutamate decarboxylase 65/67 (GAD65/67) expression in BDNF deficient mice, leading to compromised inhibitory neurotransmission and consequent disruption of motor control[62].

BDNF deficiency also amplifies neuroinflammatory responses in the brain through multiple interconnected mechanisms. Accumulating evidence indicates that BDNF suppresses NF-κB nuclear translocation via activation of the TrkB mediated PI3K/Akt signaling pathway, thereby attenuating the release of pro-inflammatory cytokines such as TNF-α, IL-6 and IL-1β[27]. In LPS induced neuroinflammation models, localized BDNF administration significantly reduces the expression of microglial activation markers[63]. Moreover, BDNF promotes the transition of microglia toward an anti-inflammatory M2 phenotype by activating STAT3 through TrkB, enhancing the secretion of anti-inflammatory mediators[64]. Clinically, reduced BDNF levels in the cerebrospinal fluid of PD patients are significantly correlated with elevated levels of pro-inflammatory cytokines, including TNF-α and IL-6[65]. Collectively, these findings indicate that BDNF deficiency disrupts the delicate balance between neuroprotective and neuroinflammatory processes, establishing a self-reinforcing pathological loop that accelerates disease progression in PD.

Proteomic analysis revealed that BDNF deficiency acts as a critical upstream event driving the aberrant activation of the TLR4 signaling pathway in the PD model. This observation is highly consistent with findings from multiple pathological models. In necrotizing enterocolitis (NEC), glial cell derived BDNF in the gut has been shown to suppress intestinal TLR4 signaling, thereby conferring protection against NEC development[66]. Furthermore, probiotic interventions have been reported to upregulate BDNF expression while simultaneously downregulate TLR4 levels[67, 68]. In the oxygen glucose deprivation (OGD) injury model, KLF2 exerts neuroprotective effects by activating the BDNF/TrkB pathway, which in turn inhibits TLR4 expression and attenuates TLR4 mediated inflammatory responses in microglia[69]. Collectively, these findings indicate that loss of BDNF relieves tonic inhibition on the TLR4 pathway, resulting in its pathological overactivation. In the context of PD, this dysregulated TLR4 signaling may stem from neuronal homeostasis disruption caused by BDNF deficiency, leading to increased release of endogenous danger associated molecular patterns (DAMPs), such as misfolded α-syn, which persistently activate TLR4 receptors on microglia[55, 70]. GsRe directly targets BDNF to enhance its inhibitory control over TLR4 signaling. Moreover, BDNF upregulation promotes microglial polarization

toward the neuroprotective M2 phenotype [71], facilitating the secretion of anti-inflammatory cytokines like IL-10 and suppressing the expression of antigen presenting molecules. This contributes to the remodeling of an anti-inflammatory microenvironment and indirectly mitigates TLR4 driven neuroinflammation[72].

In the BDNF cKO PD model, WDFY1 protein expression was significantly upregulated. As a critical adaptor protein in the TLR3/4 signaling pathway[73], WDFY1 anchors to early endosomal membranes via its FYVE domain and recruits the downstream adaptor TRIF, thereby robustly activating the NF-κB and IRF3 signaling pathways and promoting the production of type I interferons and pro-inflammatory cytokines[74, 75]. This study demonstrates that BDNF deficiency relieves the tonic negative regulation of WDFY1, resulting in aberrant activation of the TLR4 pathway and microglial hyperactivation, key events that constitute the core mechanism of the BDNF deficiency/TLR4 inflammatory axis. This finding aligns with reports of specific WDFY1 upregulation in the brain tissue of schizophrenia patients[76], suggesting that dysregulation of the BDNF//WDFY1/TLR4 axis may represent a shared pathological mechanism across multiple neuropsychiatric disorders. However, emerging evidence indicates that PRDX6 suppresses neurogenesis by downregulating WDFY1 and TLR4 signaling[77], highlighting the essential role of the WDFY1/TLR4 axis in neural plasticity and underscoring the necessity for precise regulatory control of its activity.

This study primarily focused on the regulatory role of BDNF on the TLR4/WDFY1 inflammatory pathway. However, our experimental design, to some extent, overlooked the modulatory effect of BDNF on its canonical receptor TrkB signaling pathway. In the context of BDNF deficiency, downstream signaling of the TrkB receptor (such as PI3K/Akt and Ras/ERK1/2) may also be affected [78] [79], which could be one of the underlying factors contributing to the abnormal expression of WDFY1/TLR4 and the activation of neuroinflammation. Furthermore, although we observed the restoration of WDFY1 and TLR4 expression following Re treatment, it remains unclear whether this recovery is partially attributable to indirect modulation of the TrkB signaling pathway. Future studies should further investigate the intersection between the canonical BDNF/TrkB signaling pathway and the noncanonical BDNF/TLR4 pathway to clarify their respective contributions within the neuroinflammatory regulatory network.

Conclusions

These results consistently indicate that under conditions of BDNF deficiency, the TLR signaling pathway is overactivated. GsRe is a key active component responsible for the neuroprotective effects of total ginseng saponins. It works by enhancing the inhibitory effect of BDNF on TLR4 and suppressing the activity of its adaptor protein WDFY1, thereby synergistically restraining the excessive activation of the TLR4/TRIF mediated NF-κB and STAT1 signaling pathways. Consequently, this reverses the polarization of microglia toward the M1 pro-inflammatory phenotype, ultimately alleviates neuroinflammation, inhibits neuronal apoptosis, blocks the transmission of pathological signals, and improves motor deficits

as well as dopaminergic neuron damage in Parkinson's disease models. This mechanism represents a crucial pathway through which GsRe exerts its neuroprotective effects.

Abbreviations

MPTP, 1-Methyl-4-phenyl-1,2,3,6-tetrahydropyridine.

MPP^+, 1-Methyl-4-phenylpyridinium ion.

α-Syn, Alpha-Synuclein.

BCL-2, B-cell Leukemia/Lymphoma-2.

Bax, BCL-2-associated X protein.

BDNF, Brain Derived Neurotrophic Factor.

Cleaved-Caspases3, Cleaved Cysteine Aspartate-Specific Protease 3.

CD206, Cluster of Differentiation 206.

CD86, Cluster of Differentiation 86.

cKO, Conditional Knock Out.

DA, Dopamine.

DAT, Dopamine Transporter.

GsRe, Ginsenoside Re.

IL-1β, Interleukin-1 Beta.

IL-10, Interleukin-10.

Iba-1, Ionized Calcium Binding Adapter Molecule 1.

NF-κB, Nuclear Factor-kappa B.

PD, Parkinson's Disease.

p-NF-κB, Phosphorylated-Nuclear Factor-kappa B.

SNpc, Substantia Nigra Pars Compacta.

TRIF, TIR Domain-containing Adapter Molecule 1.

TLR4, Toll Like Receptor 4.

GS, Total Ginsenosides.

TGF-β, Transforming Growth Factor-beta.

TrkB, Tropomyosin Receptor Kinase B.

TNF-α, Tumor Necrosis Factor-Alpha.

TH, Tyrosine Hydroxylase.

WDFY1, WD40 Repeat and FYVE Containing Protein 1.

WT, Wild Type.

Declarations

Funding

The Shanghai Pujiang Program, China (Grant Number 23PJ1412300) as well as The Project of "Taking on Challenges and Accepting Responsibilities" of the Seventh People's Hospital of Shanghai University of Traditional Chinese Medicine (Grant Number QYCXZY250303).

Authors` Contributions

M.T., F.Z. and Z.L. were responsible for drafting the initial manuscript. J.T. and D.G. contributed by offering editorial support, writing guidance, and valuable suggestions. The final version of the manuscript was reviewed and approved by J.G., W.G. and Z.Y. prior to submission. All authors played a role in the conception and submission of the manuscript.

Ethics Approval and Consent to Participate

All experimental procedures involving animals were conducted in accordance with the guidelines approved by the Institutional Animal Care and Use Committee of Changchun University of Chinese Medicine (Ethics Approval Number: 2025929).

Competing Interest

All authors declare that the research was conducted in the absence of any commercial or financial relationships that could be construed as a potential conflict of interest.

Availability of Data and Materials

The datasets used and/or analyzed during the current study are available from the corresponding author on reasonable request.

Consent for Publication

Not applicable.

Graphical Abstract

In PD, GsRe crosses the blood brain barrier and potentiates BDNF signaling in dopaminergic neurons. Enhanced BDNF/TrkB activation subsequently suppresses microglial TLR4 signaling, leading to downregulation of the downstream WDFY1/TRIF/NF-κB/STAT1 inflammatory cascade. This multimodal mechanism attenuates chronic neuroinflammation, mitigates dopaminergic neuronal apoptosis, restores striatal dopamine homeostasis, and ultimately ameliorates motor deficits. Collectively, these findings underscore the BDNF/TLR4 axis as a pivotal regulator of neuro-immune crosstalk in PD pathogenesis and position GsRe as a promising disease-modifying candidate for therapeutic development.

References

1. Wang Y, Wei X, Wang H, Zhang Y, Li P, Zhou Y, et al. Ginsenoside Rg1 alleviates cognitive impairment in vascular dementia by modulating Adcy1/Kdr–mediated cholinergic synapse and PI3K–AKT pathway. Phytomedicine. 2025;143:156882.
2. Huang Q, Su H, Qi B, Wang Y, Yan K, Wang X, et al. A SIRT1 Activator, Ginsenoside Rc, Promotes Energy Metabolism in Cardiomyocytes and Neurons. J Am Chem Soc. 2021;143:1416–27.
3. Li TY, Chen JX, Xie ZY, Fang JS, Wu QQ, Cao XY, et al. Ginsenoside Ro ameliorates cognitive impairment and neuroinflammation in APP/PS1 mice via the IBA1/GFAP-MAPK signaling pathway. Front Pharmacol. 2025;16:1528590.
4. Chen HY, Dong MM, He HH, Piao XM, Han X, Li RX, et al. Ginsenoside Re Prevents Depression-like Behaviors via Inhibition of Inflammation, Oxidative Stress, and Activating BDNF/TrkB/ERK/CREB Signaling: An In Vivo and In Vitro Study. J Agric Food Chem. 2024;72:19838–51.
5. Liu S, Zhang Y, Zhou H, Ma YT, Huang FZ, Lei TY, et al. Ginsenoside Re Inhibits NLRP3 Inflammasome Activation in Depressive Mice by Promoting PINK1-Mediated Mitophagy. J Agric Food Chem. 2025;73:10934–46.
6. Tang X, Zhu M, Zhu Z, Tang W, Zhang H, Chen Y, et al. Ginsenoside Re inhibits non-small cell lung cancer progression by suppressing macrophage M2 polarization induced by AMPKα1/STING positive feedback loop. Phytother Res. 2024;38:5088–106.
7. Wang H, Lv J, Jiang N, Huang H, Wang Q, Liu X. Ginsenoside Re protects against chronic restraint stress-induced cognitive deficits through regulation of NLRP3 and Nrf2 pathways in mice. Phytother Res. 2021;35:2523–35.
8. Cai JS, Huang KL, Han SN, Chen RC, Li ZJ, Chen Y, et al. A comprehensive system review of pharmacological effects and relative mechanisms of Ginsenoside Re: Recent advances and future perspectives. Phytomedicine. 2022;102:154119.

9. Morris HR, Spillantini MG, Sue CM, Williams-Gray CH. The pathogenesis of Parkinson's disease. Lancet. 2024;403:293–304.
10. Altar CA, Boylan CB, Jackson C, Hershenson S, Miller J, Wiegand SJ et al. ,. *Brain-derived neurotrophic factor augments rotational behavior and nigrostriatal dopamine turnover in vivo. Proceedings of the National Academy of Sciences 1992; 89: 11347-51.*
11. Toader C, Serban M, Munteanu O, Covache-Busuioc R-A, Enyedi M, Ciurea AV, et al. From Synaptic Plasticity to Neurodegeneration: BDNF as a Transformative Target in Medicine. Int J Mol Sci. 2025;26:4271.
12. Akbari M, Gholipour M, Hussen BM, Taheri M, Eslami S, Sayad A, et al. Expression of BDNF-Associated lncRNAs in Parkinson's disease. Metab Brain Dis. 2022;37:901–9.
13. Yuan Y, Sun J, Zhao M, Hu J, Wang X, Du G, et al. Overexpression of α-Synuclein Down-Regulates BDNF Expression. Cell Mol Neurobiol. 2010;30:939–46.
14. Miller KM, Patterson JR, Kochmanski J, Kemp CJ, Stoll AC, Onyekpe CU, et al. Striatal Afferent BDNF Is Disrupted by Synucleinopathy and Partially Restored by STN DBS. J Neurosci. 2021;41:2039–52.
15. Kang SS, Zhang Z, Liu X, Manfredsson FP, Benskey MJ, Cao X et al. ,. *TrkB neurotrophic activities are blocked by α-synuclein, triggering dopaminergic cell death in Parkinson's disease. Proc. Natl. Acad. Sci. U. S. A. 2017; 114: 10773-8.*
16. Palasz E, Wysocka A, Gasiorowska A, Chalimoniuk M, Niewiadomski W, Niewiadomska G. BDNF as a Promising Therapeutic Agent in Parkinson's Disease. Int J Mol Sci. 2020;21:1170.
17. Dluzen DE, Anderson LI, McDermott JL, Kucera J, Walro JM. Striatal dopamine output is compromised within +/- BDNF mice. Volume 43. New York, N.Y.): Synapse; 2002. pp. 112–7.
18. Heidari A, Yazdanpanah N, Rezaei N. The role of Toll-like receptors and neuroinflammation in Parkinson's disease. J Neuroinflammation. 2022;19:135.
19. Stefanova N, Fellner L, Reindl M, Masliah E, Poewe W, Wenning GK. Toll-Like Receptor 4 Promotes α-Synuclein Clearance and Survival of Nigral Dopaminergic Neurons. Am J Pathol. 2011;179:954–63.
20. Conte C, Roscini L, Sardella R, Mariucci G, Scorzoni S, Beccari T, et al. Toll Like Receptor 4 Affects the Cerebral Biochemical Changes Induced by MPTP Treatment. Neurochem. Res. 2017;42:493–500.
21. Xue F, Zhang M, Zhao R-Y, Wang X-W, Gu Y, Yang Y, et al. Dectin-1 participates in neuroinflammation and dopaminergic neurodegeneration through synergistic signaling crosstalk with TLR4. Brain Behav Immun. 2025;126:260–73.
22. Campolo M, Paterniti I, Siracusa R, Filippone A, Esposito E, Cuzzocrea S. TLR4 absence reduces neuroinflammation and inflammasome activation in Parkinson's diseases in vivo model. Brain Behav Immun. 2019;76:236–47.
23. Meng X-w, Gao J-l, Zuo J-L, Wang L-N, Liu S-l, Jin X-H, et al. Toll-like receptor-4/p38 MAPK signaling in the dorsal horn contributes to P2X4 receptor activation and BDNF over-secretion in cancer induced bone pain. Neurosci Res. 2017;125:37–45.

24. Rahimifard M, Maqbool F, Moeini-Nodeh S, Niaz K, Abdollahi M, Braidy N, et al. Targeting the TLR4 signaling pathway by polyphenols: A novel therapeutic strategy for neuroinflammation. Ageing Res Rev. 2017;36:11–9.
25. Muscat SM, Deems NP, Butler MJ, Scaria EA, Bettes MN, Cleary SP, et al. Selective TLR4 Antagonism Prevents and Reverses Morphine-Induced Persistent Postoperative Cognitive Dysfunction, Dysregulation of Synaptic Elements, and Impaired BDNF Signaling in Aged Male Rats. J Neurosci. 2023;43:155–72.
26. Caviedes A, Lafourcade C, Soto C, Wyneken U. BDNF/NF-κB Signaling in the Neurobiology of Depression. Curr Pharm Des. 2017;23:3154–63.
27. Dadkhah M, Baziar M, Rezaei N. The regulatory role of BDNF in neuroimmune axis function and neuroinflammation induced by chronic stress: A new therapeutic strategies for neurodegenerative disorders. Cytokine. 2024;174:156477.
28. Yang Y, Han C, Guo L, Guan Q. High expression of the HMGB1-TLR4 axis and its downstream signaling factors in patients with Parkinson's disease and the relationship of pathological staging. Brain Behav. 2018;8:e00948.
29. Nikitina MA, Koroleva ES, Brazovskaya NG, Boyko AS, Levchuk LA, Ivanova SA et al. *,. Associations of serum neuromarkers with clinical features of Parkinson's disease. Zh. Nevrol. Psikhiatr. Im. S. S. Korsakova 2024; 124: 145 – 52.*
30. Chen H, Dong M, He H, Piao X, Han X, Li R, et al. Ginsenoside Re Prevents Depression-like Behaviors via Inhibition of Inflammation, Oxidative Stress, and Activating BDNF/TrkB/ERK/CREB Signaling: An In Vivo and In Vitro Study. J Agric Food Chem. 2024;72:19838–51.
31. Oh J, Kwon TW, Choi JH, Kim Y, Moon S-K, Nah S-Y, et al. Ginsenoside-Re inhibits experimental autoimmune encephalomyelitis as a mouse model of multiple sclerosis by downregulating TLR4/MyD88/NF-κB signaling pathways. Phytomedicine. 2024;122:155065.
32. Nair A, Jacob S. A simple practice guide for dose conversion between animals and human. J Basic Clin Pharm. 2016;7:27–31.
33. Xiao S, Liu L, Qin X, Xu L, Chai Z, Li Z. Cycloastragenol targets Fpr2 to inhibit the TLR4/NF-κB signaling pathway and alleviate neuroinflammation in Parkinson's disease. Phytomedicine. 2025;139:156462.
34. Liu SL, Yang Y, Zong Y, Chen WJ, Geng JN, Zhao Y et al. Ginsenoside Rg3 alleviates brain damage caused by chlorpyrifos exposure by targeting and regulating the microbial-gut-brain axis. Phytomedicine 2025; 143.
35. Qin B-F, Gao S, Feng Q-y, Chen W, Sun H-M, Song J. Regulation of Nur77-TLR4/MyD88 signaling pathway is required for Ginsenoside Rc ameliorates hepatic fibrosis regression by deactivating hepatic stellate cells. Acta Histochem. 2023;125:152079.
36. Fang C, Wang L, Qiao J, Chang L, He Q, Zhang X, et al. Differential regulation of lipopolysaccharide-induced IL-1β and TNF-α production in macrophages by palmitate via modulating TLR4 downstream signaling. Int Immunopharmacol. 2022;103:108456.

37. Chong GE. We don't need no inflammation. Nat Chem Biol. 2024;20:657.
38. Li XH, Fu NS, Xing ZM. MiR-100 suppresses inflammatory activation of microglia and neuronal apoptosis following spinal cord injury via TLR4/NF-κB pathway. Eur Rev Med Pharmacol Sci. 2019;23:8713–20.
39. Nandakumar R, Paludan SR. Catching the adaptor-WDFY1, a new player in the TLR-TRIF pathway. EMBO Rep. 2015;16:397–8.
40. Xiong M, Xia DH, Yu HL, Meng LX, Zhang XY, Chen JH et al. Microglia Process α-Synuclein Fibrils and Enhance their Pathogenicity in a TREM2-Dependent Manner. Adv Sci 2025; 12.
41. Fernández-Arjona MD, Grondona JM, Fernández-Llebrez P, López-Avalos MD. Microglial activation by microbial neuraminidase through TLR2 and TLR4 receptors. J Neuroinflammation 2019; 16.
42. Chien LH, Deng JS, Jiang WP, Chou YN, Lin JG, Huang GJ. Evaluation of lung protection of Sanghuangporus sanghuang through TLR4/NF-κB/MAPK, keap1/Nrf2/HO-1, CaMKK/AMPK/Sirt1, and TGF-β/SMAD3 signaling pathways mediating apoptosis and autophagy. Biomed Pharmacother. 2023;165:115080.
43. Zhou S, Liu Y, Liu Y, Duan Z, Zhu CA-O, Wang P, et al. Ginsenoside Rk3 Alleviates Neuroinflammation and Gastrointestinal Dysfunction in Parkinson's Disease via Modulation of Gut Microbiota-Mediated Butyric Acid Metabolism. J Agric Food Chem. 2025;73(38):24139–54.
44. Wang SS, Peng Y, Fan PL, Ye JR, Ma WY, Wu QL, et al. Ginsenoside Rg1 ameliorates stress-exacerbated Parkinson's disease in mice by eliminating RTP801 and α-synuclein autophagic degradation obstacle. Acta Pharmacol Sin. 2025;46:308–25.
45. Ding YY, Botchway BOA, Zhang Y, Liu XH. Ginsenosides can target brain-derived neurotrophic factor to improve Parkinson's disease. Food Funct. 2023;14:5537–50.
46. Li J, Zhao G, Yu C, Qu Y, Shen X, Zhao Y, et al. Ginsenoside Re exerts neuroprotective in MPTP mice: potential links to gut microbiota and serum metabolism. Neuropharmacology. 2026;282:110596.
47. González-Burgos E, Fernández-Moriano C, Lozano R, Iglesias I, Gómez-Serranillos MP. Ginsenosides Rd and Re co-treatments improve rotenone-induced oxidative stress and mitochondrial impairment in SH-SY5Y neuroblastoma cells. Food Chem Toxicol. 2017;109:38–47.
48. Qiao J, Zhao Y, Liu Y, Zhang S, Zhao W, Liu S, et al. Neuroprotective effect of Ginsenoside Re against neurotoxin–induced Parkinson's disease models via induction of Nrf2. Mol Med Rep. 2022;25:215.
49. Zhao Y-N, Shao X, Ouyang L-F, Chen L, Gu L. Qualitative detection of ginsenosides in brain tissues after oral administration of high-purity ginseng total saponins by using polyclonal antibody against ginsenosides. Chin J Nat Med. 2018;16:175–83.
50. Manocha GD, Floden AM, Puig KL, Nagamoto-Combs K, Scherzer CR, Combs CK. Defining the contribution of neuroinflammation to Parkinson's disease in humanized immune system mice. Mol Neurodegener. 2017;12:17.
51. Yang L, Huang H, Fan Y, Xu L, Jin X, Xiao B, et al. Astragaloside IV ameliorates Parkinson's disease by inhibiting TLR4/ NF-κB-dependent neuroinflammation. Int Immunopharmacol. 2025;160:114972.

52. Somensi N, Lopes SC, Gasparotto J, Gonçalves RM, Tiefensee-Ribeiro C, Peixoto DO, et al. Role of toll-like receptor 4 and sex in 6-hydroxydopamine-induced behavioral impairments and neurodegeneration in mice. Neurochem Int. 2021;151:105215.
53. da Rocha Sobrinho HM, da Silva DJ, Gomides LF, Dorta ML, Pelli de Oliveira MA, Ribeiro-Dias F. TLR4 and TLR2 activation is differentially associated with age during Parkinson's disease. Immunol Invest. 2018;47:71–88.
54. Šneiderienė G, Czekalska MA, Xu CK, Jayaram AK, Krainer G, Arter WE, et al. α-Synuclein Oligomers Displace Monomeric α-Synuclein from Lipid Membranes. ACS Nano. 2024;18:17469–82.
55. Hughes CD, Choi ML, Ryten M, Hopkins L, Drews A, Botia JA, et al. Picomolar concentrations of oligomeric alpha-synuclein sensitizes TLR4 to play an initiating role in Parkinson's disease pathogenesis. Acta Neuropathol. 2019;137:103–20.
56. Cheng Z, Taylor B, Ourthiague DR, Hoffmann A. Distinct single-cell signaling characteristics are conferred by the MyD88 and TRIF pathways during TLR4 activation. Sci Signal. 2015;8:ra69–ra.
57. Bellucci A, Bubacco L, Longhena F, Parrella E, Faustini G, Porrini V, et al. Nuclear Factor-κB Dysregulation and α-Synuclein Pathology: Critical Interplay in the Pathogenesis of Parkinson's Disease. Front Aging Neurosci. 2020;12:68.
58. Xiong L, Zhu H, Liu J, Wang R, Zhong T, Jiang X, et al. Design and synthesis of novel derivatives of bisepoxylignans as potent anti-inflammatory agents involves the modulation of the M1/M2 microglia phenotype via TLR4/NF-κB signaling pathway. Eur J Med Chem. 2025;282:117092.
59. Choi SE, Park YS, Koh HC. NF-κB/p53-activated inflammatory response involves in diquat-induced mitochondrial dysfunction and apoptosis. Environ Toxicol. 2018;33:1005–18.
60. Boger HA, Mannangatti P, Samuvel DJ, Saylor AJ, Bender TS, McGinty JF, et al. Effects of brain-derived neurotrophic factor on dopaminergic function and motor behavior during aging. Genes Brain Behav. 2011;10:186–98.
61. Rantamaki T, Kemppainen S, Autio H, Staven S, Koivisto H, Kojima M, et al. The Impact of Bdnf Gene Deficiency to the Memory Impairment and Brain Pathology of APPswe/PS1dE9 Mouse Model of Alzheimer's Disease. PLoS ONE. 2013;8:e68722.
62. Li H, Lin LY, Zhang Y, Lim Y, Rahman M, Beck A, et al. Pro-BDNF Knockout Causes Abnormal Motor Behaviours and Early Death in Mice. Neuroscience. 2020;438:145–57.
63. Wu SY, Pan BS, Tsai SF, Chiang YT, Huang BM, Mo FE, et al. BDNF reverses aging-related microglial activation. J Neuroinflammation. 2020;17:210.
64. Bi CL, Fu YL, Li B. Brain-derived neurotrophic factor alleviates diabetes mellitus-accelerated atherosclerosis by promoting M2 polarization of macrophages through repressing the STAT3 pathway. Cell Signal. 2020;70:109569.
65. Lindqvist D, Hall S, Surova Y, Nielsen HM, Janelidze S, Brundin L, et al. Cerebrospinal fluid inflammatory markers in Parkinson's disease - Associations with depression, fatigue, and cognitive impairment. Brain Behav Immun. 2013;33:183–9.

66. Kovler ML, Salazar AJG, Fulton WB, Lu P, Yamaguchi Y, Zhou QJ, et al. Toll-like receptor 4-mediated enteric glia loss is critical for the development of necrotizing enterocolitis. Sci Transl Med. 2021;13:eabg3459.
67. Thabet E, Dief AE, Arafa SAF, Yakout D, Ali MA. Antibiotic-induced gut microbe dysbiosis alters neurobehavior in mice through modulation of BDNF and gut integrity. Physiol Behav. 2024;283:114621.
68. Mohammed SK, Magdy YM, El-Waseef DAA, Nabih ES, Hamouda MA, El-kharashi OA. Modulation of hippocampal TLR4/BDNF signal pathway using probiotics is a step closer towards treating cognitive impairment in NASH model. Physiol Behav. 2020;214:112762.
69. Zhou JB, Wang MC, Deng DF. KLF2 protects BV2 microglial cells against oxygen and glucose deprivation injury by modulating BDNF/TrkB pathway. Gene. 2020;735:144277.
70. Gorecki AM, Anyaegbu CC, Anderton RS. TLR2 and TLR4 in Parkinson's disease pathogenesis: the environment takes a toll on the gut. Transl Neurodegener. 2021;10:47.
71. Komori T, Okamura K, Ikehara M, Yamamuro K, Endo N, Okumura K, et al. Brain-derived neurotrophic factor from microglia regulates neuronal development in the medial prefrontal cortex and its associated social behavior. Mol Psychiatry. 2024;29:1338–49.
72. Zhang JQ, Rong PJ, Zhang LJ, He H, Zhou T, Fan YH, et al. IL4-driven microglia modulate stress resilience through BDNF-dependent neurogenesis. Sci Adv. 2021;7:eabb9888.
73. Hu Y-H, Zhang Y, Jiang L-Q, Wang S, Lei C-Q, Sun M-S, et al. WDFY1 mediates TLR3/4 signaling by recruiting TRIF. EMBO Rep. 2015;16:447–55.
74. Li D, Lai J, Du H, Liu B, Hu C, Li M. Grass carp (Ctenopharyngodon idella) WDFY1 activates IFN1 response via TLR3-TRIF-IRF3 axis. Fish Physiol. Biochem. 2025; 51: 131.
75. Ning F, Li X, Yu L, Zhang B, Zhao Y, Liu Y, et al. Hes1 attenuates type I IFN responses via VEGF-C and WDFY1. J Exp Med. 2019;216:1396–410.
76. Sancho-Balsells A, Brito V, Fernandez B, Pardo M, Straccia M, Gines S, et al. Lack of Helios During Neural Development Induces Adult Schizophrenia-Like Behaviors Associated With Aberrant Levels of the TRIF-Recruiter Protein WDFY1. Front Cell Neurosci. 2020;14:93.
77. Yeo IJ, Park MH, Son DJ, Kim JY, Nam KT, Hyun BK, et al. PRDX6 Inhibits Neurogenesis through Downregulation of WDFY1-Mediated TLR4 Signal. Mol Neurobiol. 2019;56:3132–44.
78. Guo LT, Wang SQ, Su J, Xu LX, Ji ZY, Zhang RY, et al. Baicalin ameliorates neuroinflammation-induced depressive-like behavior through inhibition of toll-like receptor 4 expression via the PI3K/AKT/FoxO1 pathway. J Neuroinflammation. 2019;16:95.
79. Xiang YX, Wei XB, Du PC, Zhao H, Liu AC, Chen YG. β-Arrestin-2-ERK1/2 cPLA2 axis mediates TLR4 signaling to influence eicosanoid induction in ischemic brain. FASEB J. 2019;33:6584–95.

Tables

Table 1 is available in the Supplementary Files section.

Figures

Figure 1

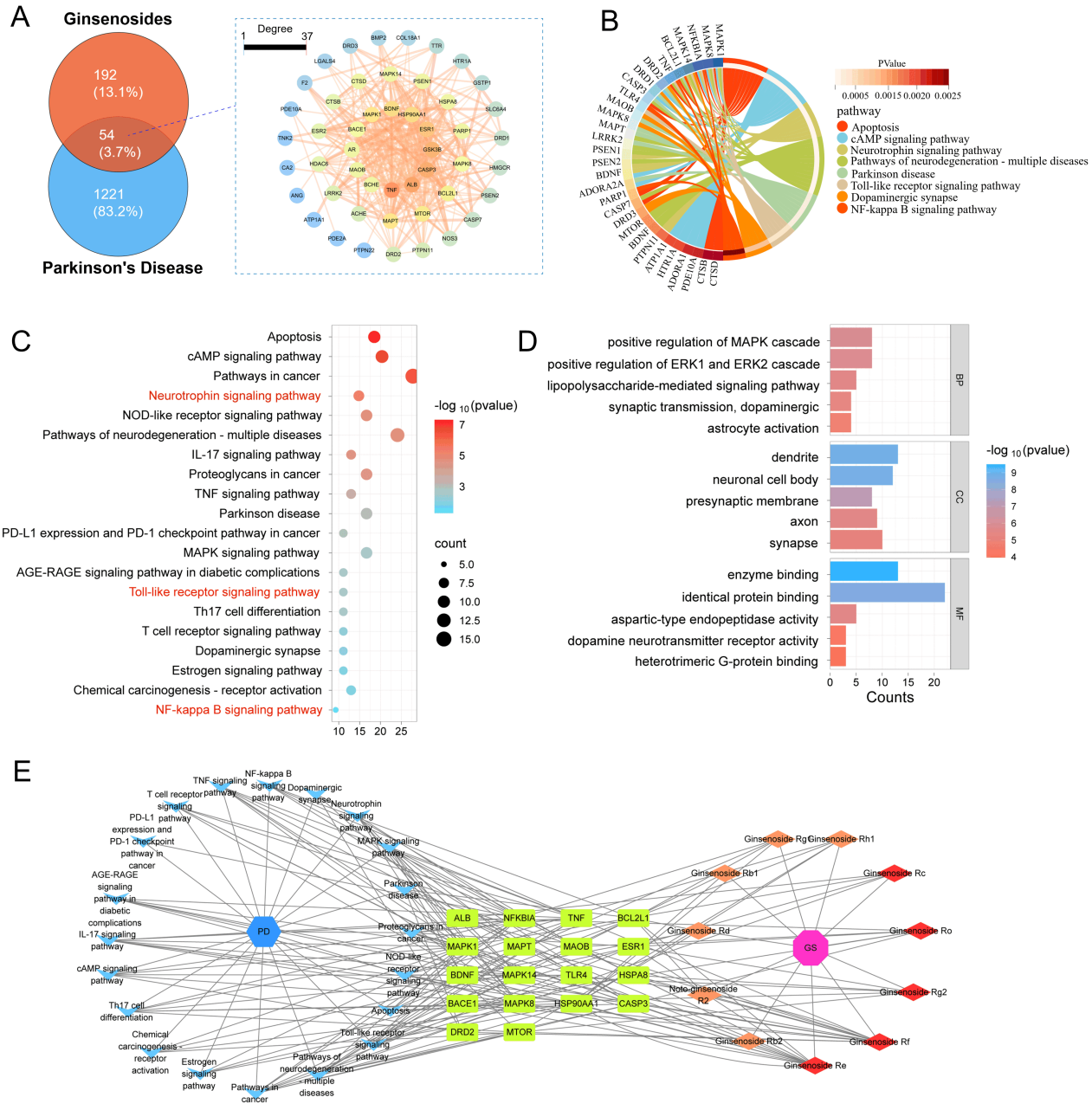


Figure 1

Chemical composition analysis of GS and network pharmacology study on the treatment of PD.

(A) Venn diagram showing the overlapping genes between bioactive compounds in GS and PD related targets. (B) Chord plot illustrates the associations between key targets and relevant signaling pathways. (C) KEGG pathway enrichment analysis of the shared genes. (D) GO enrichment analysis of overlapping genes. (E) Integrated network visualization of GS compounds key targets pathways PD. Compounds, targets, and pathways are represented by orange diamonds, yellow squares, and green inverted triangles, respectively.

Figure 2

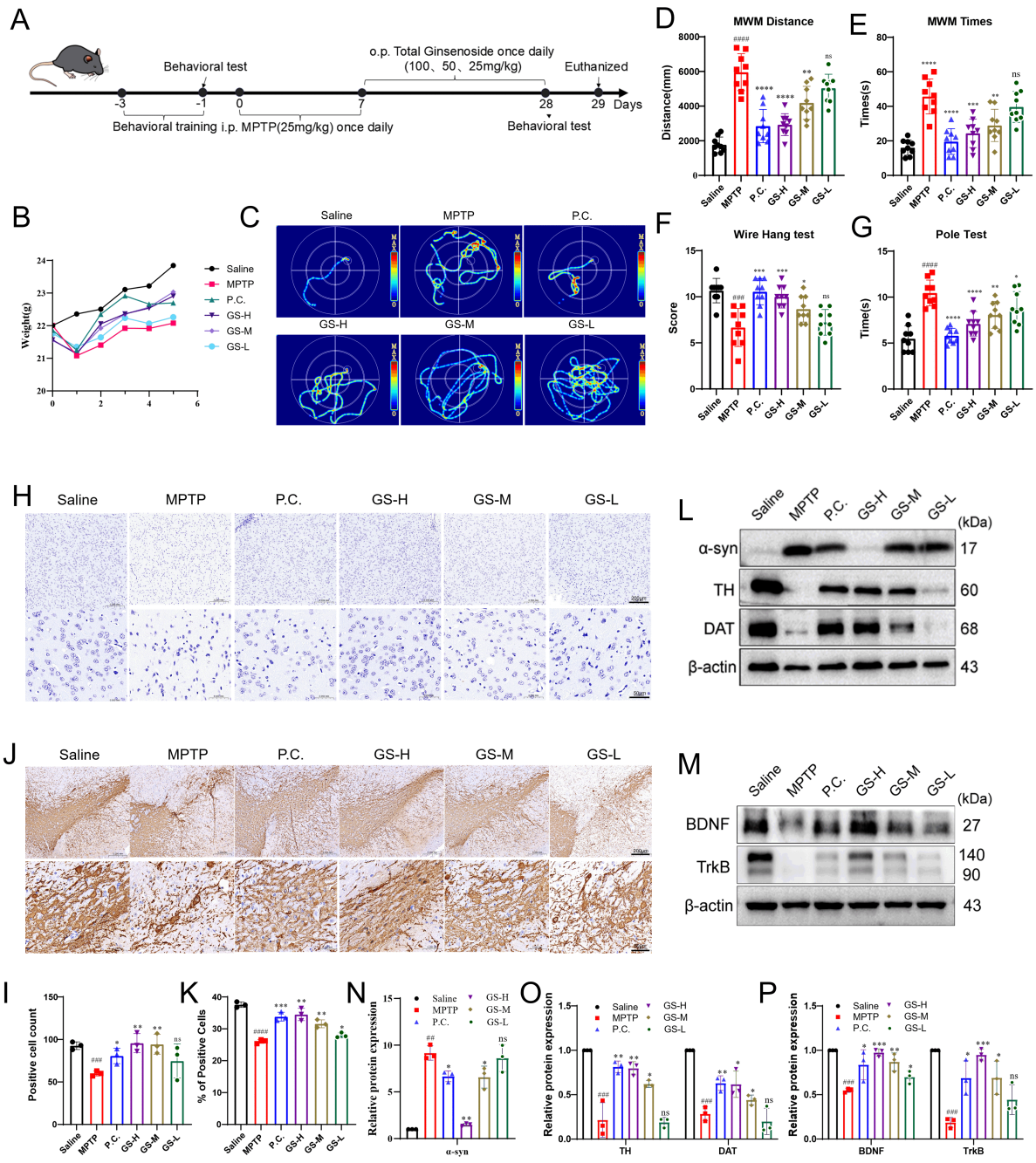


Figure 2

GS ameliorate motor dysfunction and neuronal damage in an MPTP induced mouse model of PD.

(A) Schematic diagram of experimental design for animal study. (B) Changes in mouse body weight (n = 9). (C–E) Heat maps of movement trajectories (C), total distance traveled (D) and time to locate the platform (E) in the Morris water maze test (n=9). (F) Statistical analysis of hanging wire test scores (n=9). (G) Movement duration in the pole test (n=9). (H–I) Representative Nissl staining images of the striatum (H) and quantitative analysis of Nissl-positive areas (I) (n=3). Scale bar: 50 μm. Microscope magnification: 40×. (J–K) Representative immunohistochemical staining images (J) and quantitative analysis (K) of TH in SNpc (n=3). Scale bar: 50 μm. Microscope magnification: 40×. (L, N–O) Representative Western blot images (L) and quantitative analysis (N–O) of α-syn, TH, and DAT protein expression levels (n=3). (M, P) Representative Western blot images (M) and quantitative analysis (P) of BDNF/TrkB protein expression levels (n=3). Compared with the Saline group: $^{\#}p < 0.05$, $^{\#\#}p < 0.01$, $^{\#\#\#}p < 0.001$. Compared with the MPTP group: $^{*}p < 0.05$, $^{**}p < 0.01$, $^{***}p < 0.001$.

Figure 3

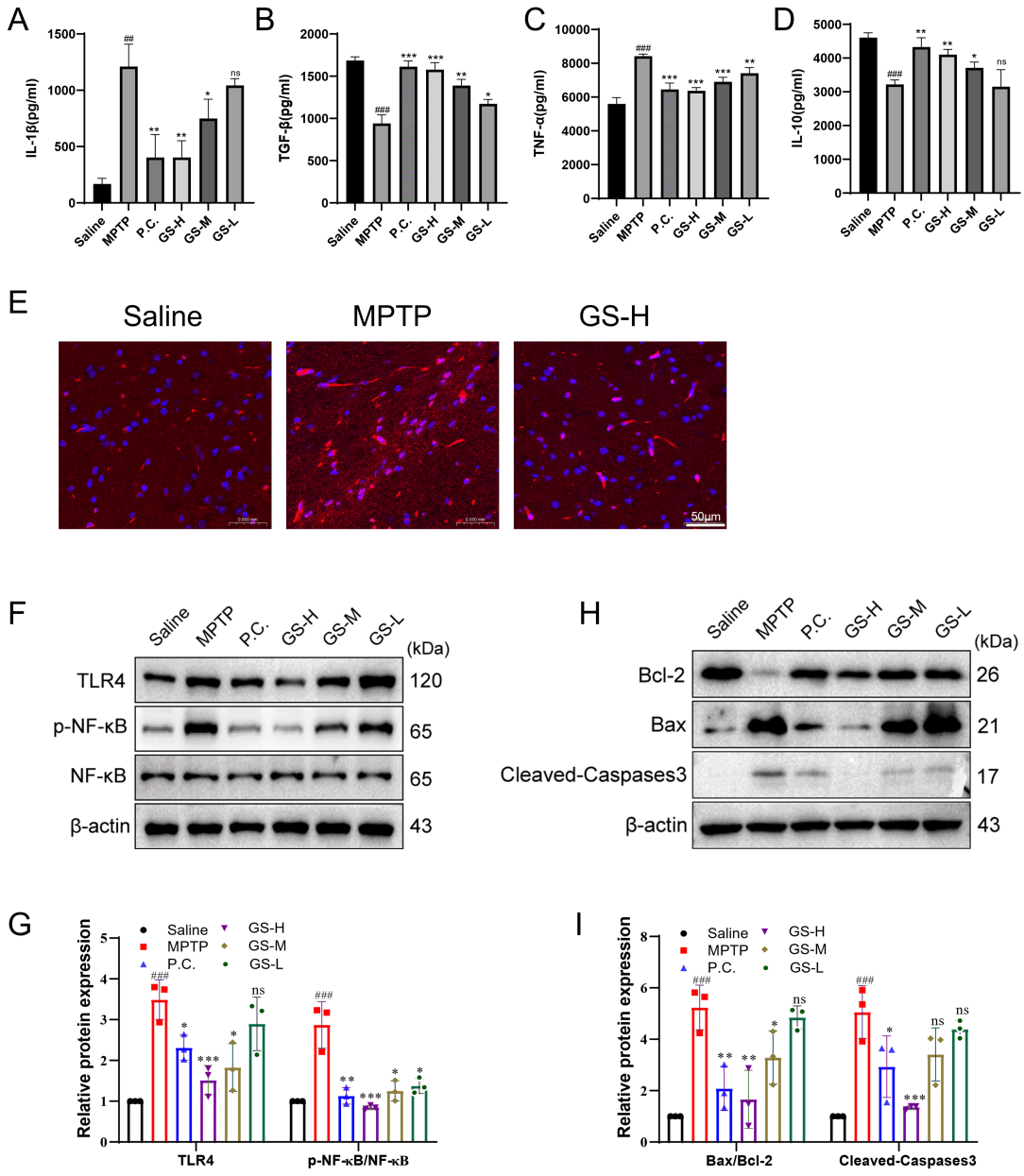


Figure 3

GS suppress MPTP induced neuroinflammation, apoptosis and activation of the TLR4/NF-κB signaling pathway.

(A–D) ELISA measurement of TNF-α (A), IL-1β (B), TGF-β (C) and IL-10 (D) expression levels in mouse brain tissue (n=6). (E) Immunofluorescence staining showing nuclear translocation of NF-κB (n=3).

Scale bar: 50 μm. Microscope magnification: 40×. (F–G) Representative Western blot images (F) and quantitative analysis (G) of TLR4, NF-κB and phosphorylated NF-κB (p-NF-κB) at Ser-529 protein expression levels (n=3). (H–I) Representative Western blot images (H) and quantitative analysis (I) of apoptosis related proteins BCL-2, Bax and cleaved caspase-3 (n=3). Compared with the Saline group: $^{\#}p < 0.05$, $^{\#\#}p < 0.01$, $^{\#\#\#}p < 0.001$. Compared with the MPTP group: $^{*}p < 0.05$, $^{**}p < 0.01$, $^{***}p < 0.001$.

Figure 4

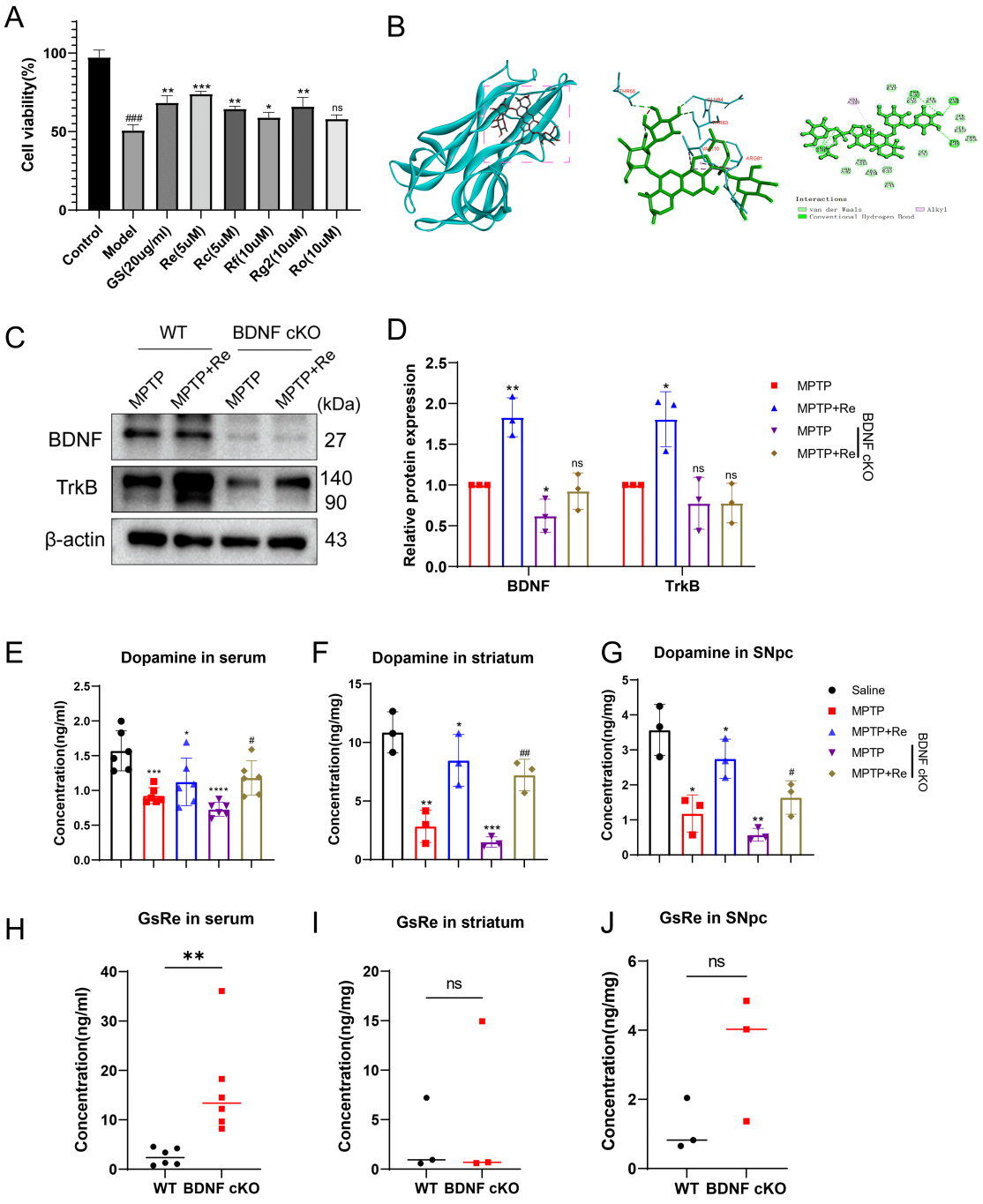


Figure 4

GsRe targets BDNF to elevate dopamine levels.

(A) Effects of different ginsenosides on cell viability in MPP^+ induced neuronal cells as determined by CCK-8 assay (n=3). (B) Molecular docking model of GsRe with BDNF. (C) Representative Western blot images and quantitative analysis of BDNF and TrkB expression levels (n=3). (D–F) Dopamine levels in serum (D), SNpc (E) and striatum (F) (n=6). (G–I) GsRe concentrations in serum (G), SNpc (H) and striatum (I) measured by LC-MS/MS (n=6). Compared with the Control group: $^{*}p < 0.05$, $^{**}p < 0.01$, $^{***}p < 0.001$. Compared with the BDNF cKO + MPTP group: $^{\#}p < 0.05$, $^{\#\#}p < 0.01$. ns, not significant.

Figure 5

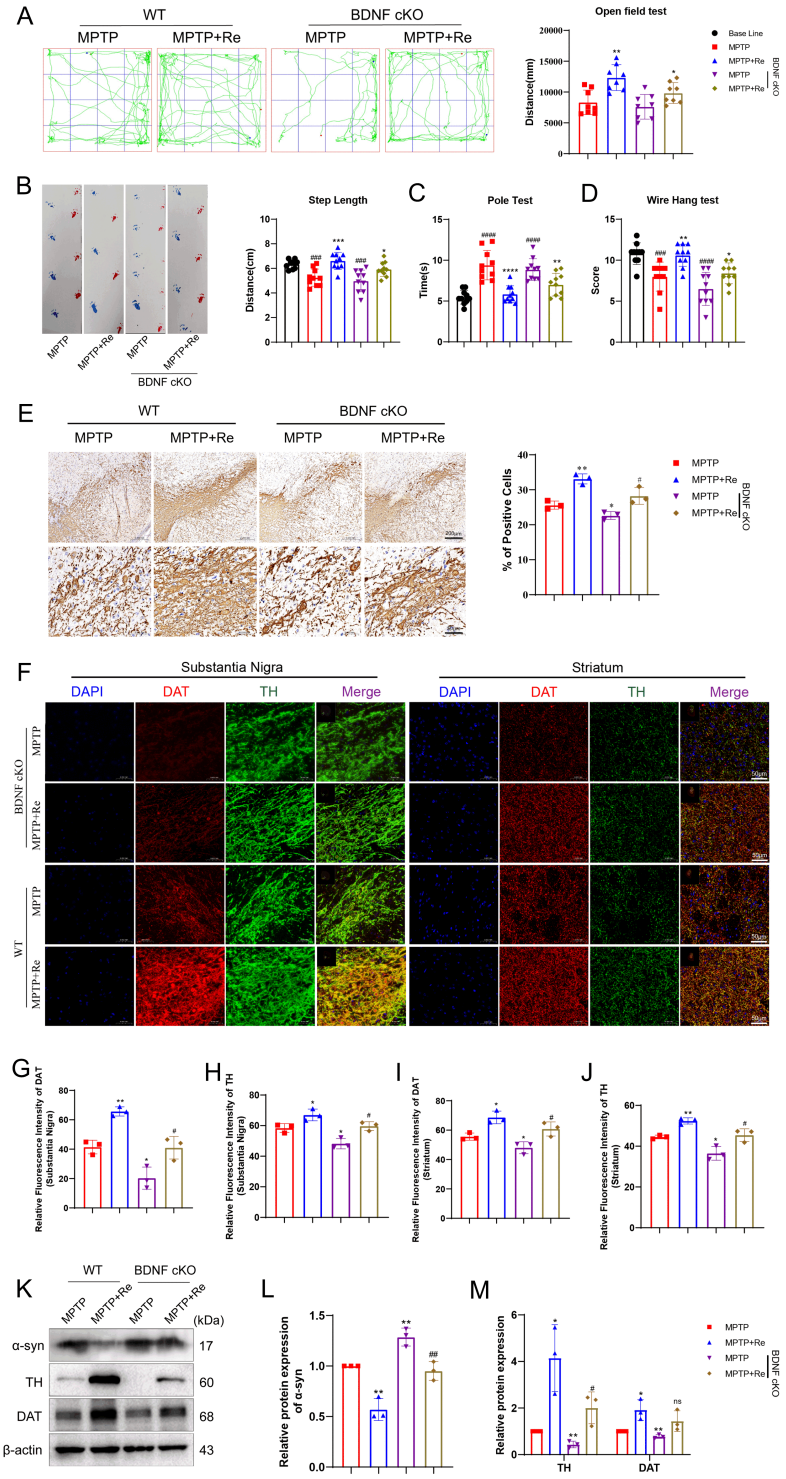


Figure 5

GsRe restores dopaminergic neuron loss in a mouse model of PD.

(A) Heat maps of movement trajectories and statistical analysis of total travel distance in the open field test over a 5-minute period (n=9). (B) Representative footprint patterns and quantitative analysis of stride length (n=9). (C) Movement duration in the pole test (n=9). (D) Hanging wire test scores (n=9).

(E) Representative immunohistochemical staining images and quantitative analysis of TH in the tissues of the SNpc (n=3). Scale bar: 50 μm. Microscope magnification: 40×. (F–J) Representative immunofluorescence images and quantitative analysis of TH and DAT expression in the SNpc and striatum (n=3). Scale bar: 50 μm. Microscope magnification: 40×. (K–M) Representative Western blot images (K) and quantitative analysis (L, M) of α-syn, TH and DAT protein expression levels (n=3). Compared with the Control group: $^{*}p < 0.05$, $^{**}p < 0.01$, $^{***}p < 0.001$. Compared with the BDNF cKO + MPTP group: $^{\#}p < 0.05$, $^{\#\#}p < 0.01$. ns, not significant.

Figure 6

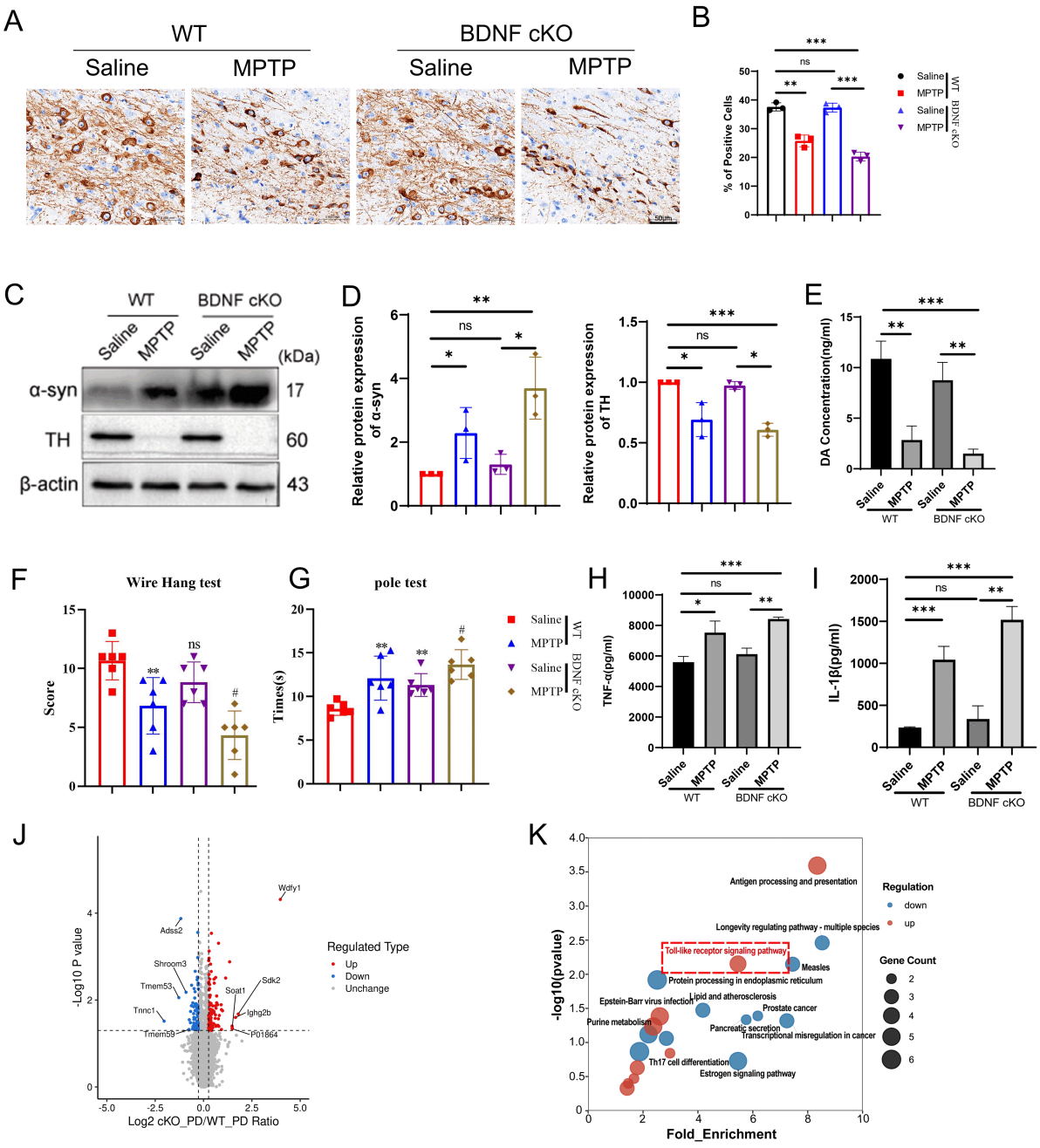


Figure 6

BDNF deficiency exacerbates PD pathology and neuroinflammation via TLR pathway activation.

(A–B) Representative immunohistochemical staining images and quantitative analysis of TH in the tissues of the SNpc (n=3). Scale bar: 50 μm. Microscope magnification: 40×. (C–D) Representative Western blot images and quantitative analysis of α-syn and TH expression levels (n=3). (E) Dopamine content in the striatum (n=6). (F) Statistical analysis of hanging wire test scores (n=9). (G) Movement duration in the pole test (n=9). (H–I) ELISA measurement of TNF-α and IL-1β expression levels in mouse brain tissue (n=6). (J) Volcano plot displaying differentially expressed proteins between BDNF cKO + MPTP and WT + MPTP groups (n=3). (K) KEGG pathway enrichment analysis of differentially expressed proteins in the BDNF cKO + MPTP versus WT+ MPTP group comparison $^{*}p < 0.05$, $^{**}p < 0.01$, $^{***}p < 0.001$.

Figure 7

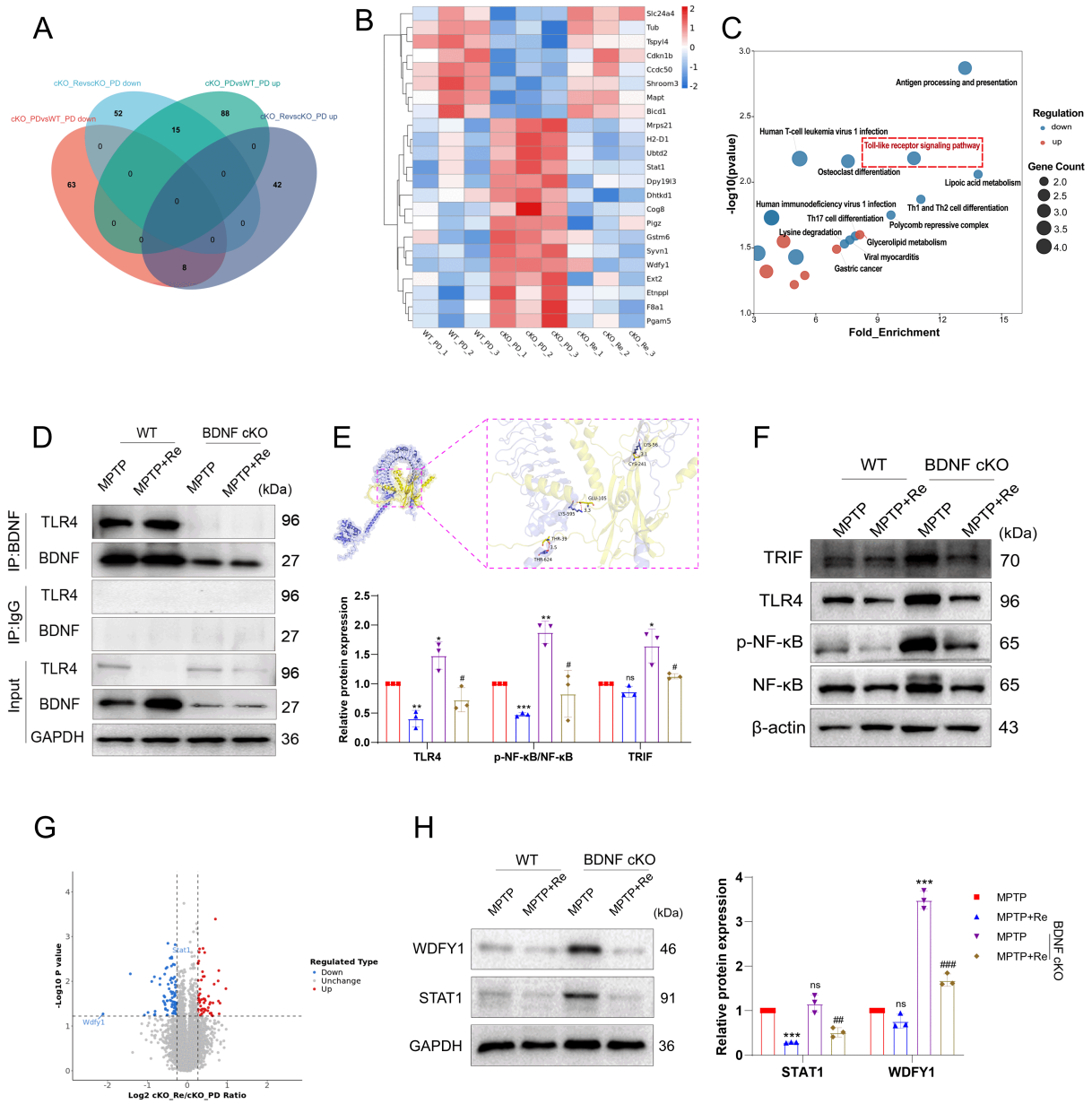


Figure 7

Proteomic analysis reveals that GsRe alleviates BDNF mediated activation of the TLR signaling pathway.

(A) Venn diagram showing the overlap of upregulated and downregulated proteins between the BDNF cKO+ MPTP versus WT+ MPTP group and BDNF cKO+ MPTP versus BDNF cKO Re group comparisons. (B) Heatmap analysis of overlapping differentially expressed proteins identified in the Venn diagram

(n=3). (C) KEGG pathway enrichment analysis of differentially expressed proteins in the BDNF cKO Re versus BDNF cKO+ MPTP group comparison. (D) PPI between BDNF and TLR4 were detected by Co-IP assay (n=3). (E) Visualization of molecular docking between BDNF and TLR4 proteins. (F) Representative Western blot images and quantitative analysis of TLR4, TRIF, NF-κB and phosphorylated NF-κB (p-NF-κB) protein expression levels (n=3). (G) Volcano plot displaying differentially expressed proteins between BDNF cKO Re versus BDNF cKO+ MPTP groups (n=3). (H) Representative Western blot images and quantitative analysis of WDFY1 and STAT1 protein expression levels (n=3). Compared with the Control group: $^{*}p < 0.05$, $^{**}p < 0.01$, $^{***}p < 0.001$. Compared with the BDNF cKO + MPTP group: $^{\#}p < 0.05$, $^{\#\#}p < 0.01$. ns, not significant.

Figure 8

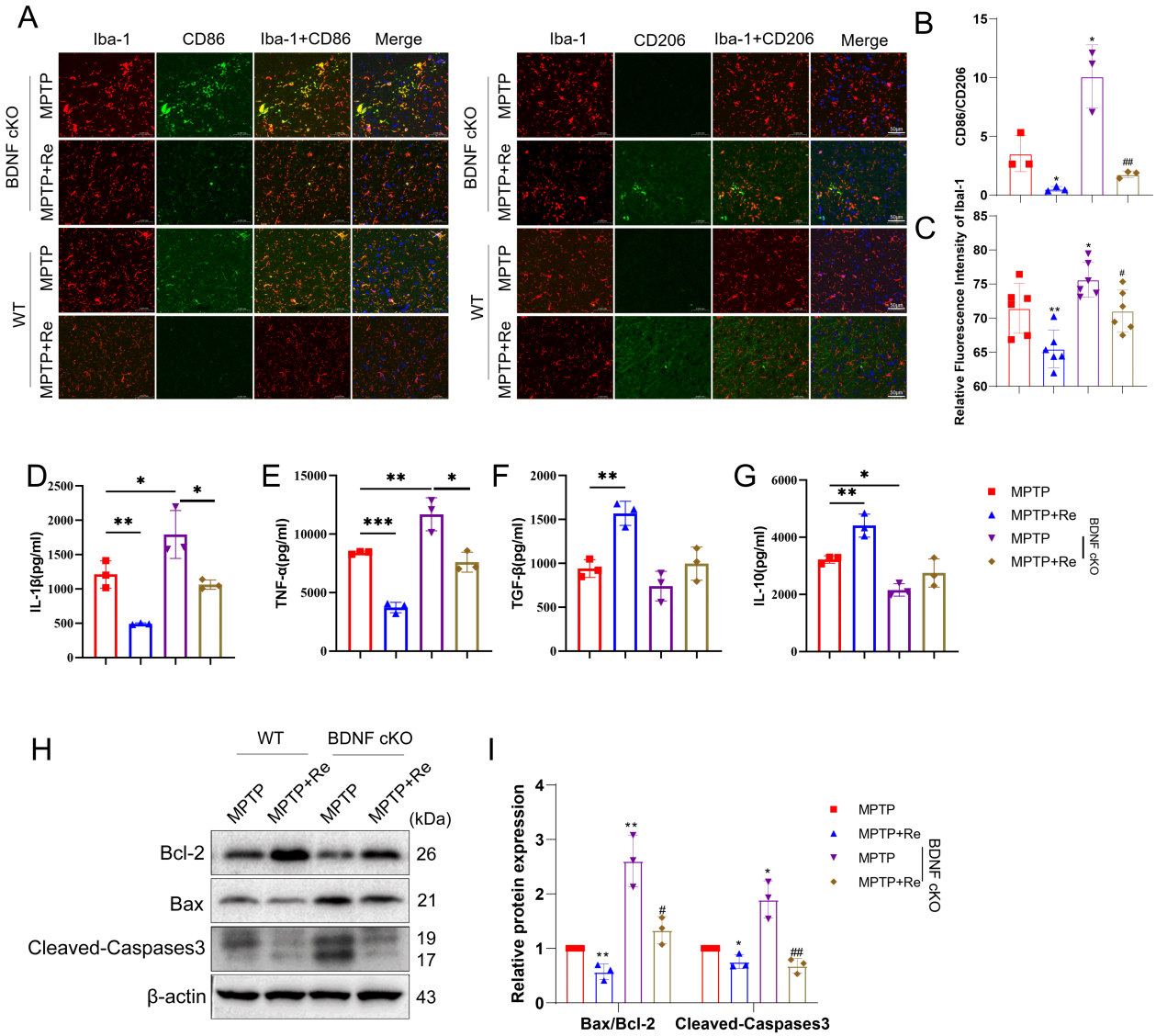


Figure 8

GsRe Inhibits TLR4 Mediated Neuroinflammation, Microglial Polarization and Neuronal Apoptosis.

(A) Representative immunofluorescence double-staining images of Iba-1⁺/CD86⁺ and Iba-1⁺/CD206⁺ cells (n = 3). (B) Ratio of CD86 to CD206 means fluorescence intensity (n=3). (C) Quantitative analysis of Iba-1 means fluorescence intensity in brain tissue (n=6). (D-G) ELISA measurement of IL-1β (D), TNF-

α(E), TGF-β (F) and IL-10 (G) expression levels in mouse brain tissue (n=3). (H-I) Representative Western blot images and quantitative analysis of apoptosis related proteins BCL-2, Bax and cleaved caspase-3 (n=3). Compared with the Control group: $^{*}p < 0.05$, $^{**}p < 0.01$, $^{***}p < 0.001$. Compared with the BDNF cKO + MPTP group: $^{\#}p < 0.05$, $^{\#\#}p < 0.01$. ns, not significant.

Supplementary Files

This is a list of supplementary files associated with this preprint. Click to download.

- Table.pdf
- SupplementaryFigure.pptx
- SupplementaryFigureLegends.docx